Informes Técnicos Ciemat

1465

Diciembre, 2019

Cadmium adsorption onto gamma-alumina nanoparticles: experimental and modelling study

U. B. Alonso de los Ríos
N. Mayordomo Herranz
T. Missana

GOBIERNO DE ESPAÑA

MINISTERIO DE CIENCIA, INNOVACIÓN Y UNIVERSIDADES

Ciemat

Centro de Investigaciones Energéticas, Medioambientales y Tecnológicas

Informes Técnicos Ciemat

1465

Diciembre, 2019

Cadmium adsorption onto gamma-alumina nanoparticles: experimental and modelling study

U. B. Alonso de los Ríos
N. Mayordomo Herranz
T. Missana

Departamento de Medio Ambiente

Publicación disponible en el Catálogo general de publicaciones oficiales.

Depósito Legal: M-26385-2011
ISSN: 1135-9420
NIPO: 693-19-051-1

Maquetación y Publicación:
Editorial CIEMAT
Avda. Complutense, 40 28040-MADRID
Correo: editorial@ciemat.es
Novedades editoriales CIEMAT

CADMIUM ADSORPTION ONTO GAMMA-ALUMINA NANOPARTICLES: EXPERIMENTAL AND MODELLING STUDY

Alonso de los Ríos, U.B; Mayordomo Herranz, N.; Missana, T.

45 pp, 55 ref, 29 figures, 4 tables

Abstract:

Cadmium is one of the heavy metals of concern, both from the point of view of public health and environmental safety, because it is a toxic element, bio-accumulative and persistent. Therefore, it is considered of vital importance to develop materials and methodologies that favour its retention and removal.

In this study, the retention of cadmium in a nanoparticulate oxide, γ-Al_2O_3 was analyzed. A complete experimental sorption study in a wide range of chemical was carried out, to elucidate the main retention mechanisms.

This study is part of a broader work, in which the sorption behaviour of mixed systems, including clay materials that would form a geochemical barrier, was analysed. For analogy with previous studies of retention of contaminants in clays, a non-electrostatic surface complexation model, mechanistic and thermodynamic-based, was selected to describe Cd retention on γ-Al_2O_3.

The developed model was tested on experimental data and allows the prediction of cadmium retention in different environmental scenarios.

ADSORCIÓN DE CADMIO EN NANOPARTÍCULAS DE GAMMA-ALÚMINA: ESTUDIO EXPERIMENTAL Y DE MODELADO

Alonso de los Ríos, U.B; Mayordomo Herranz, N.; Missana, T.

45 pp, 55 ref, 29 figuras, 4 tablas

Resumen:

El cadmio es uno de los metales pesados que más preocupa, tanto desde el punto de vista de salud pública como ambiental, por ser un elemento altamente tóxico, bio-acumulable y persistente. Se considera de vital importancia desarrollar materiales y metodologías que favorezcan su retención y eliminación del medioambiente.

En este trabajo, se ha analizado la retención de cadmio en un óxido nanoparticulado, γ-Al_2O_3. Se ha realizado un completísimo estudio experimental de sorción, en un amplio rango de condiciones químicas, para elucidar los principales mecanismos de retención.

Este estudio forma parte de un trabajo mucho más amplio, en el que se ha analizado el comportamiento de sorción del cadmio en sistemas mixtos, que incluyen materiales arcillosos que conformarían una barrera geoquímica.

para describir la sorción de Cd en γ-Al_2O_3 se ha elegido un modelo de complejación no electrostático (NEM), con base termodinámica, por analogía con estudios previos de retención de contaminantes en arcillas, ,. El modelo desarrollado permite predecir la retención de cadmio en γ-Al_2O_3 en diferentes escenarios ambientales.

ACKNOWLEDGMENTS

This study was partially by the European Union within the Joint Programme on Radioactive Waste Management (EURAD), grant agreement 847593. Luis Gutiérrez Nebot is acknowledged for XRD analyses and CIEMAT Chemical Division is acknowledged for ICP analyses.

TABLE OF CONTENTS

LIST OF FIGURES

LIST OF TABLES

1 INTRODUCTION

Cadmium is one of the heavy metals of higher health and environmental concern because it is toxic to human, plants and animals, even being present at a trace level [1] and it is bio-accumulative and persistent in the environment. Cadmium naturally occurs in the environment but it also enters from electroplating, pigments, alloy manufacturing, plastic stabilizers, batteries, fertilizers, pesticides, mining, textile operations and refining industries [2, 3].

Different approaches and adsorbents are proposed for cadmium removal, like precipitation, ion exchange, solvent extraction or adsorption minerals, clays and oxides and, amongst different sorbents, gamma alumina (γ-Al_2O_3) has been proposed [4]. The acid-base properties of oxides are the main reason for its wide applications for contaminant removal [5].

In nature, γ-Al_2O_3 is found only under high pressure and high temperature conditions. However, the surface of this mineral completely hydrates, and it is considered that the hydrated surface of γ -Al_2O_3 is similar to aluminum hydroxide minerals commonly found in soils, such as gibbsite, bayerite, and boehmite [6]. The γ-Al_2O_3 is structurally different to α-Al_2O_3 because it contains both AlO_6 octahedra and AlO_4 tetrahedra in its structure.

For both economic and environmental reasons, there is an increasing demand for non-invasive and improved removal technologies [7]. The use of nanoparticles (NPs) is growing because, due to their high surface area, they can significantly increase the retention capacity and selectivity for pollutants and reactivity. In this study we propose that γ-Al_2O_3 NPs are good candidates to enhance cadmium retention.

Previous studies on Cd sorption onto Al_2O_3 are available [8-13], and also specifically on Al_2O_3 nanoparticles [10, 14, 15]. Available studies usually described Cd sorption onto Al_2O_3 by inner-sphere complexation of Cd^{2+} [12, 16] but $CdOH^+$ complexation is sometimes considered. A two-step adsorption process for cadmium metal ion (Cd^{2+}) on aluminum oxide has been also proposed: a very rapid adsorption of cadmium metal ion to the external surface followed by possible slow intra-particle diffusion in the interior of the adsorbent [9].

Cadmium adsorption onto oxides, as other cationic metals, generally exhibits pH dependency and it is influenced by the presence of competing cations or complexing ligands [15, 17]. In a general way, competition depends on the relative energies of interaction between the ions and the sorbent surface, the concentrations of the competing ions and solution pH [18]. Cations like calcium, magnesium, and other trace metal were found to reduce cadmium adsorption [18] and other authors pointed out low Cd sorption at low pH due to the competition between H^+/Na^+ and Cd^{2+} on the surface sites [15]. Sorption of halogen ions on Al_2O_3 surface was reported [19], and surface complexation constants for some mayor anions have been provided [12, 20].

However, from previous studies three main open questions were identified. First, available sorption models may fail to predict Cd sorption behaviour at trace level Cd concentrations. All reported studies were carried out with initial Cd concentration higher than µM. None of the available models provided information on more than one surface site, as observed for Cd sorption on other oxides

[18]. There are usually a small number of strong sites which are first filled, because they have higher sorption affinity, and experiments are better identified at low tracer concentration. The presence of strong sites for Cd sorption on Al_2O_3 NPs surface may be identified by carrying out experiments with Cd concentrations lower than µM.

Second, there is controversy regarding the need to include Cd- chloride complexes to describe cadmium sorption. Some authors considered that cation adsorption may be promoted in chloride-bearing fluids [11] but other authors concluded that chloride complexing lowered Cd sorption on Al_2O_3 [8]. Comparable sorption experiments carried out in absence and in presence of Cl ion, may help clarifying this issue. In fact, the contribution of other major anions, usually present in the environment, like carbonates, sulfates or nitrates is still not fully described.

Last, to the best of our knowledge, none of the reported studies provided a surface complexation model able to predict cadmium retention in a wide range of environmental conditions.

In this study, cadmium sorption onto alumina nanoparticles was deeply analysed. A combined experimental and modelling methodology was followed going for a mechanistic approach to describe surface/solution interaction by surface complexation model [21, 22]. Experiments were carried out with ^{109}Cd to improve Cd detection at low Cd concentration. Tests were carried out in different electrolytes, accounting for the presence of different ions (Cl^-, ClO_4^-, NO_3^-, SO_4^{2-}), in a wide range of experimental conditions. In fact, it has been already proven that anion sorb onto this alumina surface [20]and compete with other anions present in solution, like selenite, for sorption sites [23, 24].

This study is part of a wider research devoted to the improvement of the retention capacity of geochemical barriers, through the addition of nanoparticles, adapted to each type of contaminant [24-26]. In particular, it was analysed whether the mixture of smectite clay and γ-Al_2O_3 nanoparticles (NPs) enhances cadmium sorption [26, 27]. In order to describe retention properties of mixed systems, verifying sorption additivity [24, 25], the fundamental description of the individual systems is absolutely required.

2 EXPERIMENTAL SET-UP

2.1 ALUMINA NANOPARTICLES: CHARACTERISATION

Gamma-aluminium oxide nanopowder with nominal size < 50 nm (Sigma Aldrich) was selected. The powder was analysed by XRD to confirm the oxide phase.

For sorption experiments, γ-Al_2O_3 suspensions were mainly prepared in $NaClO_4$ of analytical grade (Merck) at ionic strengths from $5 \cdot 10^{-4}$ M to $2 \cdot 10^{-1}$ M.

To analyse the effect of electrolyte ions on Cd sorption, γ-Al_2O_3 suspensions were also prepared in $NaNO_3$, $NaHCO_3$ and Na_2SO_4 electrolytes.

The particle size and morphology were analysed by atomic force microscopy (AFM) with a Multimode (Digital Instrument) apparatus by depositing a drop of the Al_2O_3 suspension in $NaClO_4$ (2 $g \cdot L^{-1}$) onto cleaved mica modified with poly-L-lysine.

Stability of γ-Al_2O_3 nanoparticles in different electrolytes was analysed elsewhere by Photon Correlation Spectrometry (PCS) and zeta potential measurements [20].

2.1.1 SOLID DISSOLUTION

To evaluate the dissolution of γ-Al_2O_3, suspensions were prepared in $NaClO_4$ 10^{-1} M (solid to liquid ratio 0.5 $g \cdot L^{-1}$) at different pH values (from pH 3 to pH 11). Tubes were maintained under continuous stirring during different times going from 5 minutes up to 20 days.

Samples were centrifuged and, after solid separation, dissolved Al^{3+} was determined by Inductively Coupled Plasma Atomic Emission Spectrometry (Varian 735 ES, AA240 FS). The obtained Al^{3+} values were used to define the solid solubility product (log K_{Al}), as below described in section 3.2.1.

2.1.2 SURFACE SITES: POTENTIOMETRIC TITRATION

Surface characterisation of γ-Al_2O_3 NPs was carried out in [20]. The N_2-BET surface area was 136 $m^2 \cdot g^{-1}$. In particular, potentiometric acid-base titrations were carried out in the absence of CO_2(g), in closed vessels and using $NaClO_4$ as background electrolyte.

Titration data was re-simulated, incorporating Al_2O_3 dissolution and Al^{3+} hydrolysis, as described for gibbsite in [28]. Thermodynamic data considered for Al was taken from [29, 30] and reactions and stability constants are included in Table 3.

2.2 CADMIUM

A $^{109}CdCl_2$ solution prepared in 10^{-1} M HCl, which contains $37 \cdot MBq \cdot mL^{-1}$ with a $CdCl_2$ carrier (500 µg $Cd \cdot mL^{-1}$) was used for sorption experiments. Cadmium-109 is a low yield fission product

with a half-life of 462.6 days, which decays by electron capture with a major gamma emission at 88 KeV. Cadmium activity was measured by gamma counting (Cobra Autogamma, Packard).

Cadmium chloride ($CdCl_2$) solutions of high purity (Merck) were used to achieve higher Cd concentrations.

To analyse the relevance of Cd-chloride complexes, some experiments were carried out, in the absence of chloride (Cl^-), with Cd perchlorate hydrate ($CdCl_2O_8{:}xH_2O$), supplied by Sigma-Aldrich.

2.3 CADMIUM SORPTION EXPERIMENTS ONTO γ-ALUMINA

Sorption experiments were mainly carried out with 0.5 $g{\cdot}L^{-1}$ γ-Al_2O_3 suspensions in $1{\cdot}10^{-1}$ M $NaClO_4$ at desired pH.

Experiments were carried out in polyethylene centrifuge tubes (10 mL) under atmospheric conditions and at room temperature.

After the radionuclide addition, the tubes were maintained in continuous stirring during 1 week. Afterwards, the samples were centrifuged (21000·g during 60 min) and three aliquots of the liquid phase were sampled for ^{109}Cd analyses. Cd activity was measured by means of a NaI γ-counter (Cobra Autogamma, Packard). The remaining solution was used to measure the pH at equilibrium.

The Cd distribution coefficient (Kd), amongst the solid and the liquid phase, was calculated with this formula:

$$K_d = \frac{C_i - C_{eq}}{C_{eq}} \cdot \frac{V}{m} \qquad (E.\ 1)$$

where C_i and C_{eq} are respectively the initial and equilibrium Cd concentration in the liquid phase, m the mass of oxide (g) and V the volume of liquid (mL).

Cadmium sorption on the centrifuge tubes was systematically checked.

2.3.1 SORPTION KINETICS

The kinetics of Cd sorption onto γ-Al_2O_3 NPs was investigated to determine the time needed to reach the steady-state for further experiments. Kinetic tests were carried out at pH 5.5 and in $NaClO_4$ 10^{-1} M. Experiments lasted from 1 hour up to 15 days.

2.3.2 SORPTION DEPENDENCE ON PH AND IONIC STRENGHT

Sorption edge experiments were carried out with γ-Al_2O_3 suspensions prepared in $NaClO_4$ electrolyte, varying the pH from 3 to 11. Experiments were carried out with three different initial Cd concentrations: $4.6{\cdot}10^{-8}$, $9.8{\cdot}10^{-6}$ and $4.9{\cdot}10^{-4}$ M, by adding $^{109}CdCl_2$ and non-radioactive CdCl when higher concentrations are required.

Main experiments were carried out at ionic strength $1 \cdot 10^{-1}$ M, but sorption edges at different ionic strengths, from $5 \cdot 10^{-4}$ to $2 \cdot 10^{-1}$ M, were also conducted. Experiments at different ionic strengths were carried out with an initial Cd concentration of $4.6 \cdot 10^{-8}$ M.

The pH of γ-Al_2O_3 suspensions was varied from pH 3 to 11, adding aliquots of HCl or NaOH 10^{-1} M. To maintain the pH value constant, the following buffer solutions, achieving a concentration of $2 \cdot 10^{-3}$ M) to stabilise these pH ranges: 2-(N-morpholino)ethane-sulphonic acid (MES, pH 5.5-6.5); 3-(N-morpholino)propanesulphonic acid (MPS, pH 6.8-7.7); Tris(hydroxymetil)aminomethane (TRIS, 7.5-8.5); 3-(cyclohexyl amino)ethanesulphonic acid (CHES, 9.0-10.0).

Some tests were carried out without buffer addition to verify if selected buffers influence Cd sorption.

Samples were maintained in continuous stirring during 1 week, afterwards centrifuged and sampled to measure the Cd concentration in solution.

2.3.3 SORPTION ISOTHERMS

The dependence of cadmium sorption onto γ-Al_2O_3 on the initial Cd concentration was analysed by in $NaClO_4$ 10^{-1} M, by varying the radionuclide concentration (10^{-9} to 10^{-3} M) at different fixed pH: 6, 6.5, 9 and 10.

Once again, to achieve higher tracer concentration ($> 1 \cdot 10^{-6}$ M), non-radioactive $CdCl_2$ was spiked in addition to the radiotracer. The separation and analysis procedure was the same above described.

2.3.4 ALUMINA AGING OR HYDRATION EFFECTS ON CADMIUM SORPTION

Some authors reported that transformation of gamma-alumina to gibbsite, or to other aluminium oxide phases, may take place, modifying sorption conditions. In this context, alumina transformation at ambient temperature may take place due to hydration and in principle, this transformation may be fast [28].

To identify aging effects, Cd sorption edges were carried out at different pH in a suspension of alumina prepared in $NaClO_4$ one day or one month before the Cd addition.

2.3.5 LIGAND SORPTION EFFECTS ON CADMIUM SORPTION

In Missana et al, 2014 [20] it was confirmed that ClO_4^-, NO_3^-, HCO_3^- and mainly $SO4^{2-}$ anions sorb onto γ-Al_2O_3 surface. Their sorption was identified by competition with selenite ions and by changes on electrostatic charge, evaluated by zeta potential measurements. The uptake of HCO_3^- ions was even confirmed by spectroscopic measurements [23]. The sorption of Cl- was studied in [25]. Therefore, it was necessary to verify whether the sorption of anions on the alumina surface had any effect on the subsequent Cd retention. To analyse this, three different set of experiments were performed.

As a first verification, the sorption of Cd was analysed in a pre-hydrated alumina prepared in deionized water and it was compared to that of pre-hydrated alumina suspended in perchlorate at

different ionic strengths. This check was carried out in a restricted pH area (4 to 5), where the surface of the alumina is positively charged and, therefore, where the anion sorption could be more relevant. Cd initial concentration in these experiments was $4.6 \cdot 10^{-8}$ M.

Secondly, special attention was paid on verifying the relevance of Cl^- on Cd sorption since, as mentioned in the introduction, it is a controversial topic. To do so, Cd sorption edges on γ-Al_2O_3 were carried out spiking with $Cd(ClO_4)_2 \cdot xH_2O$ (and acidulated with $HClO_4$) and its retention was compared to that of $^{109}CdCl$, both with an initial Cd concentration of $9.8 \cdot 10^{-6}$. In the first case, Cd concentrations in solution were measured by Inductively Coupled Plasma Atomic Emission Spectrometry (Varian 735 ES, AA240 FS), while ^{109}Cd was measured by gamma counting (Cobra Autogamma, Packard).

Third, sorption edges were carried out in other electrolytes at 10^{-3} M ionic strength. Cd sorption was analysed in $NaNO_3$, acidulating with HNO_3 and in Na_2SO_4 acidulating with H_2SO_4. Studies with Na_2CO_3 were limited to the region of interest for carbonates, accounting for two different carbonate concentrations (10^{-2} and 10^{-1} M). Cd initial concentration was in all cases $4.6 \cdot 10^{-8}$ M.

3 SORPTION MODELLING: GENERAL CONSIDERATIONS

The aim of the study was to provide a thermodynamic sorption model, for cadmium sorption on γ-Al_2O_3 NPs, with predictive capacity in a wide range of environmental conditions. Experiments were thoroughly planned in different chemical conditions to identify the retention mechanisms.

To develop a robust surface complexation model (SCM), as described in [21, 22] and references there-in, we need: (1) to define the cadmium aqueous speciation; (2) to describe the solid surface characteristics and (3) to identify the different species or complexes involved in the contaminant retention.

With all available information, simpler or more complex surface complexation models can be proposed. Selected model (either electrostatic or non-electrostatic, double or triple layer, etc.) must be sufficiently justified by experimental results. The different hypotheses should be checked by fitting experimental data, by a trial and error procedure and, as far as possible, they must be verified. At the end, selected model must be capable of simulating the whole experimental data. In this study, the geochemical code Chess was used for the calculations [31].

3.1 CADMIUM AQUEOUS SPECIATION

A thorough review of available thermodynamic databases for cadmium species was carried out [30, 32-35].

The selected stability and formation constants for Cd aqueous and solid species are respectively gathered in Table 1 and Table 2.

In the tables, cadmium aqueous and solid species are included, with their definition and corresponding stability constants. The first column shows the equilibrium constants initially included in the geochemical chess code [31], which corresponds to values reported in [30]. In the second column, the values included are those reported in the latest IUPAC revision [33]. In the last column, the selected values are highlighted, which mainly correspond to the IUPAC revision [33] and some missing values (mainly nitrates) taken from [36].

Special attention was paid on the equilibrium constants of cadmium chloride aqueous complexes [32], nitrate complexes [36] and mainly cadmium solid phases, including carbonates [35]. In fact, the formation constants for $Cd(OH)_2(s)$ and otavite ($CdCO_3(s)$) were modified, adopting the value proposed in [35], in agreement with the experimental sorption data, as will be later discussed.

Cadmium aqueous speciation was checked. Geochemical calculations were carried out with CHESS code [31] considering experimental conditions used in sorption experiments.

AQUEOUS SPECIES	DEFINITION	logK Chess	logK	logK Selected
Cd[2+]	**Main specie**			
Cl[-]	1 HCl(aq), -1 H[+]	-0,67		-0,67
H[+]	1 H_2O, -1 OH[-]	-14		-14
HCO_3[-]	1 H[+], 1 CO_3[2-]	10,3288		10,3288
HPO_4[2-]	1 H[+], 1 PO_4[3-]	12,3218		12,3218
CdOH [+]	1 Cd[2+], 1 H_2O, -1 H[+]	-10,0751	-9.91 ± 0.1	-9,91
$Cd(OH)_2$(aq)	1 Cd[2+], 2 H_2O, -2 H[+]	-20,3402	-20.19 ±0.13	-20,19
$Cd(OH)_3$[-]	1 Cd[2+], 3 H_2O, -3 H[+]	-33,2852	-33.5 ± 0.5	-33,5
$Cd(OH)_4$[2-]	1 Cd[2+], 4 H_2O, -4 H[+]	-47,3303	-47.28 ± 0.15	-47,28
Cd_2OH[3+]	2 Cd[2+], 1 H_2O, -1 H[+]	-9,3851	-8.73 ± 0.01	-8,73
$Cd_4(OH)_4$[4+]	4 Cd[2+], 4 H_2O, -4 H[+]	-362,126	-31,8	-31,8
$CdHCO_3$[+]	1 Cd[2+], 1 HCO_3[-]	1,5	0.84-2.4	1,5
$CdCO_3$(aq)	1 Cd[2+], 1 HCO_3[-], -1 H[+]	-7,3288	-5,9288	-5,9288
$Cd(CO_3)_2$[2-]	1 Cd[2+], 2 HCO_3[-], -2H[+]	-14,2576	-14,4576	-14,4576
CdCl[+]	1 Cd[2+], 1 Cl[-]	2,7059	1.98 ± 0.06	1,98
$CdCl_2$(aq)	1 Cd[2+], 2 Cl[-]	3,3384	2.64 ± 0.09	2,64
$CdCl_3$[-]	1 Cd[2+], 3 Cl[-]	2,7112	2.3 ± 0.21	2,3
Cd(OH)Cl(aq)	1 Cd[2+], 1 Cl[-], 1 H_2O, -1 H[+]	-7,43	n.d.	n.c.
$CdSO_4$(aq)	1 Cd[2], 1 SO_4[2-]	0,0028	2.36 ± 0.04	2,36
$Cd(SO_4)_2$[2-]	1 Cd[2], 2 SO_4[2-]	n.d.	3.32 ± 0.16	3,32
$CdHPO_4$(aq)	1 Cd[2+], 1 HPO_4[2-]	n.d.	2.85 ± 0.2	2,85
CdH_2PO_4[+]	1 Cd[2], 2 HPO_4[2-], -1 H_2O	n.d.	7,9654	7,9654
CdP_2O_7[2-]	1 Cd[2], 2 H_2PO_4[2-], -1 H_2O	4,8094		4,8094
$CdNO_3$[+]	1 Cd[2+], 1 NO_3[-]	0,91	n.d.	0.41**
$Cd(NO_3)_2$	1 Cd[2+], 2 NO_3[-]	n.d.	n.d.	0.0**

*Table 1. Stability constants for Cd aqueous species accounting for the presence of major inorganic ligands OH^-, Cl^-, HCO_3^-,SO_4^{2-}, PO_4^{2-}. Three different logK values are included from Chess code database [30, 31], from IUPAC revision [33] and selected values (** data from [36]). N.d. = no data.*

Cd Solids	Definition	logK	logK	logK
Cd	1 Cd[2+], -2 H[+], -0.5O_2(aq), 1 H_2O	-56,6	n.d.	-56,6
$Cd(OH)_2$	1 Cd[2+], -2 H[+], 2 H_2O	-13,7382	-13.72 ± 0.12	-14.35**
Monteponite	1 Cd[2+], -2 H[+], 1 H_2O	-15,0972	n.d.	-15,0972
CdO©				
Otavite CdCO3(s)	1 Cd[2+], 1 HCO_3[-], -1 H[+]	1,7712	1,7336	0.5**
Cd(OH)Cl	1 Cd[2+], 1 Cl[-], -1 H[+], 1H_2O	-3,54	n.d.	-3,54
CdCl2	1 Cd[2+], 2 Cl[-]	0,6474	n.d.	0,6474
$CdCl_2$:H_2O	1 Cd[2+], 2 Cl[-], 1 H_2O	1,6747	n.d.	1,6747
$Cd_3(SO_4)(OH)_4$	3 Cd[2], 1 SO_4[2-], -4 H[+], 4 H_2O	-22,5735	n.d.	-22,5735
$Cd_3(SO_4)_2(OH)_2$	3 Cd[2], 2 SO_4[2-], -2 H[+], 2 H_2O	-6,718	n.d.	-6,718
$CdSO_4$	1 Cd[2], 1 SO_4[2-]	0,1061	n.d.	0,1061
$CdSO_4$:H_2O	1 Cd[2], 1 SO_4[2-], 1 H_2O	1,6529	n.d.	1,6529
$CdSO_4$:2.667H_2O	2 Cd[2], 1 SO_4[2-], 2.667 H_2O	1,8015	n.d.	1,8015
$Cd_3(PO_4)_2$	3 Cd[2+], 2 HPO_4[2-], -2 H[+]	7,8943		7,8943
$Cd_5H_2(PO_4)4H_2O$	5 Cd[2+], 4 HPO_4[2-], 4 H_2O, -2 H[+]	n.d.	30.9 ± 0.3	30,9

*Table 2. Formation constants for Cd solids considering presence of main inorganic ligands OH^-, Cl^-, HCO_3^-,SO_4^{2}, PO_4^{2-}. Three different logK values are included from Chess code database [30, 31], from IUPAC revision [33] and selected values (** data from [36]). n.d = no data.*

3.2 SOLID SURFACE DESCRIPTION

3.2.1 ALUMINA SOLUBILITY PRODUCT

Dissolution experiments were carried out to evaluate the concentration of dissolved Al^{3+} in different conditions. Measured values were used to determine the solubility product ($logK_{Al}$).

In the Chess code, the equation is defined by the following equilibrium:

$$2Al^{3+} + 3H_2O \Leftrightarrow Al_2O_3 + 6H^+ \qquad logK_{Al} \qquad (E.\ 2)$$

This equilibrium equation is generally described, considering the formation constant ($logK_f$), as follows:

$$2Al(s) + \frac{3}{2}O_2(aq) \Leftrightarrow Al_2O_3 \qquad logK_f \qquad (E.\ 3)$$

This formation constant can be calculated through thermodynamic enthalpies of formation (ΔH) or free-Gibbs energies (ΔG_f) by:

$$\Delta G = \Delta H - T\Delta S = RTln(10) \cdot logK_f \qquad (E.\ 4)$$

where R is the gas constant and T the temperature (298.5 K, in our case).

Solubility product and formation constants can be compared using the following equations and constants [29].

$$2H^+ + 2e^- + 0.5O_2 \Leftrightarrow H_2O \qquad logK = -41.546 \qquad (E.\ 5)$$

$$Al^{3+} + 3e^- \Leftrightarrow Al(s) \qquad logK = -84.22 \qquad (E.\ 6)$$

3.2.2 ALUMINA SURFACE SITES

Metal oxides have functional surface hydroxyl groups (≡SOH) capable to form bonds. Surface complexation on these groups is considered responsible for ion sorption.

It is usually assumed that hydroxyl groups in oxides are amphoteric and develop a pH-dependent charge at the edge sorption sites, by protonation / deprotonation reactions.

In this study, two different surface hydroxyl groups, with different Cd affinity were considered. They are defined as weak (≡S_wOH) and strong (≡S_sOH) sites. Both surface groups undergo de/ protonation according to the following equilibria:

$$\equiv S_wOH_2^+ \underset{pK_{wa1}}{\Longleftrightarrow} \equiv S_wOH + H^+ \qquad (E.\ 7)$$

$$\equiv S_wOH \underset{pK_{wa2}}{\Longleftrightarrow} \equiv S_wO^- + H^+ \qquad (E.\ 8)$$

$$\equiv S_sOH_2^+ \underset{pK_{sa1}}{\Longleftrightarrow} \equiv S_sOH + H^+ \qquad (E.\ 9)$$

$$\equiv S_sOH \underset{pK_{sa2}}{\Longleftrightarrow} \equiv S_sO^- + H^+ \qquad (E.\ 10)$$

where ≡ S_wOH and ≡ S_sOH represent neutral surface sites, ≡ $S_wOH_2^+$ and ≡ $S_sOH_2^+$ are positively charged sites, and ≡ S_wO^- and≡ S_wO^- are negatively charged surface sites.

K_{wa1}, K_{sa1} , K_{wa2} and K_{sa2} are apparent acidity constants, for weak and strong sites, that can be defined:

$$K_{a1} = \frac{(\equiv SOH)\gamma_H(H^+)}{(\equiv SOH_2^+)} \cdot exp(-\frac{F\Psi}{RT}) \qquad (E.\ 11)$$

$$K_{a2} = \frac{(\equiv SO^-)\gamma_H(H^+)}{(\equiv SOH)} \cdot exp(-\frac{F\Psi}{RT}) \qquad (E.\ 12)$$

where (·) represent molar concentrations, γ_H the activity coefficient for H^+ and exp(-FΨ/RT) accounts for the electrostatic term, which actually was not considered in the present work.

Activity coefficients were corrected with Davies equation:

$$log\gamma_H = -Az^2\left(\frac{\sqrt{I}}{1+\sqrt{I}} - 0.3I\right) \qquad (E.\ 13)$$

Potentiometric titration data was used to determine the total concentration of weak sites available per unit amount of solid (sites·nm^{-2}) and their apparent acidity constants.

3.2.2.1 Surface sites: Potentiometric titration simulation

Potentiometric titrations were carried out in a previous study [20] where data was fitted discarding γ-Al_2O_3 dissolution.

In this study, solid dissolution is accounted for and titration data was re-simulated. In fact, during normal continuous titration, H^+/OH^- consumption can increase by dissolution of the solid phase [37]. For the modelling, Al^{3+} hydrolysis reactions were accounted for the acid–base balance in solution. Selected species, reactions and constants [28] are summarised in Table 3

SPECIES	MASS LOW AND BALANCE EQUATIONS	LOGK	REFERENCE
γ-Al_2O_3(s)	$2Al^{3+} + 3H_2O \leftrightarrow Al_2O_3 + 6H^+$	-16	This work
$AlOH^{2+}$	$Al^{3+} + H_2O \leftrightarrow AlOH^{2+} + H^+$	-4,957	[29]
$Al(OH)_2^+$	$Al^{3+} + 2H_2O \leftrightarrow Al(OH)_2^+ + 2H^+$	-10,5945	[29]
$Al(OH)_3$	$Al^{3+} + 3H_2O \leftrightarrow Al(OH)_3^0 + 3H^+$	-16,432	[29]
$Al(OH)_4^-$	$Al^{3+} + 4H_2O \leftrightarrow Al(OH)_4^- + 4H^+$	-22,879	[29]
$Al_2(OH)_2^{4+}$	$2Al^{3+} + 2H_2O \leftrightarrow Al_2(OH)_2^{4+} + 2H^+$	-7,6982	[30]
$Al_3(OH)_4^{5+}$	$3Al^{3+} + 4H_2O \leftrightarrow Al_3(OH)_4^{5+} + 4H^+$	-13,8803	[30]

Table 3. Mass balance equations and equilibrium constants for γ-Al_2O_3(s) and for selected Al hydrolysed species [29, 30, 38].

The concentration of weak sites (N_w), was determined from fitting of potentiometric titration data and the concentration of strong sites (N_s), was obtained by a trial procedure to better fit the Cd isotherms. Selected values are included in Table 4.

The surface charge is given by the proton excess or proton deficiency at the surface.

$$\sigma\left(\frac{AS}{F}\right) = (\equiv SOH_2^+) - (\equiv SO^-) = F[\Gamma_H - \Gamma_{OH}] \qquad (E.\ 14)$$

F is the Faraday constant, A the specific surface area (m^2·g^{-1}), S the solid concentration (g·L^{-1}), and Γ_H and Γ_{OH} are experimental sorption densities (mol·m^{-2}) of H^+ and OH^-.

Titrations were carried out under anoxic conditions and it is assumed that protons H^+ are the only specifically sorbing ions. The excess of protons at the surface (positive charge) by the addition of a known acid concentration (Ca in M) and the proton deficit (negative charge) caused by addition of base concentration (Cb in M) can be obtained by the following equation [28]:

$$Ca - Cb = TOT\ H = (H^+) - (OH^-) + 3(Al^{3+}) + 2(AlOH^{2+}) + (Al(OH)_2^+) - (Al(OH)_4^-) + 4(Al_2(OH)_2^{4+}) + 5\left(Al_3(OH)_4^{5+}\right) + (\equiv AlOH_2^+) - (\equiv AlO^-) \qquad (E.\ 15)$$

The total number of surface sites is defined by:

$$TOT\ (\equiv SOH) = \ (\equiv SOH_2^+) + (\equiv SOH^0) + (\equiv SO^-) \qquad (E.\ 16)$$

3.3 CADMIUM SURFACE COMPLEXATION ON ALUMINA SURFACE

Cadmium sorption onto γ-Al_2O_3 NPs was described considering a two-site non-electrostatic surface complexation model.

As mentioned before, none of the available Cd sorption studies onto Al_2O_3 considered a two site model, but it is widely accepted that there are more than one type of aluminium surface hydroxyl group [39]. The difference between the different types of surface groups primarily depends upon the number of aluminium atoms to which the hydroxyl is bond, as well as on the coordination of the aluminium ion (octahedral or tetrahedral).

3.3.1 METAL SORPTION

The availability of free ≡SOH groups is an essential requirement for the sorption process. Figure 1 presents represents the possible surface complexes that can take place on aluminium oxide surface [28].

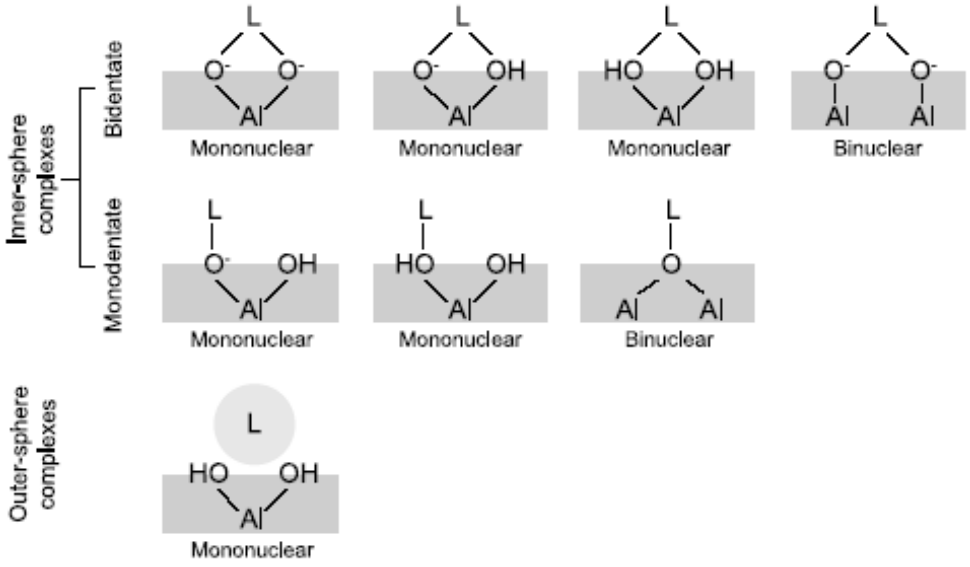

Figure 1. Schematic representation of possible surface complexes [28].

Specific adsorption of cations can take place by inner-sphere complexation at the Al_2O_3 surface on functional groups as described by the following equation:

$$(\equiv SOH) + M^{z+} \Leftrightarrow (\equiv SO)M^{z-1} + H^+ \qquad (E.\ 17)$$

It is considered that **s**imultaneous cation adsorption and hydrolysis can occur. Sorption of hydroxylated forms of the metal, in both weak and strong sites, and can be defined by:

$$(\equiv SOH) + M^{z+} + H_2O \Leftrightarrow (\equiv SO)MOH^{z-2} + 2H^+ \qquad (E.\ 18)$$

In addition, it is often taken into account that more than one proton is released to solution per metal ion (M^{z+})adsorbed and bi-(tri)- n nuclear bonding is postulated [18].

Metal bound to one Al hydroxyl site is denoted ≡ AlOH (weak or strong). Likewise, when bound to two or three Al ions the hydroxyl is referred to as double (≡ Al_2OH), triple (≡ Al_3OH) or n-coordinated ≡ Al_nOH, described like:

$$(\equiv S_nOH) + M^{z+} \Leftrightarrow (\equiv S)_nOM^{z-1} + nH^+ \qquad (E.\ 19)$$

In some cases, the metal ions are simultaneously attached to two surface hydroxyl groups. Cadmium bidentate (n = 2) complexes would be defined as follows:

$$n(\equiv SOH) + M^{z+} \Leftrightarrow (\equiv SO)_nM^{z-1} + nH^+ \qquad (E.\ 20)$$

3.3.2 LIGAND COMPETITION AND TERNARY COMPLEXES

The perchlorate, nitrate, bicarbonate and sulphate adsorption on alumina surface was also included in the model, considering the reactions and constants obtained on the same solid, which were experimentally determined in [20] and for Cl- in [24]. Spectroscopic analyses also confirmed carbonate sorption on alumina surface (Mayordomo et al, 2018). Other authors also included sorption of halogen ions on Al_2O_3 [12, 19]. Selected values are included in Table 4.

The reactions between anionic ligands (L^{n-}) and alumina positive surface sites can be defined as:

$$SOH_2^+ + L^{n-} \overset{K}{\Leftrightarrow} SOH_2\ L^{n-} \qquad (E.\ 21)$$

This definition does not disagree with the description of a non-electrostatic model.

In this gamma-alumina, unexpected cation adsorption was systematically measured at pH < 5, for example for Sr^{2+} [25]. In the Sr sorption study, this contribution to Sr sorption, with a logKd (mL g^{-1}) ≈ 2) was empirically included in the model, to be rigorous with the theoretical basis of a non-electrostatic model.

In any case, metal cation (M^{z+}) uptake by γ-Al_2O_3 by co-adsorption with electrolyte anions (L^{n-}: ClO_4^-, SO_4^{2-}) onto amphoteric positive surface sites (≡SOH_2) can be hypothesized, considering the formation of ternary surface species (≡SOH_2-ClO_4-Cd^{2+}), (≡SOH_2-SO_4-Cd^{2+}), and (≡SOH_2-NO_3-Cd). These reactions can be described as:

$$(\equiv AlOH_2) + L^{n-} + M^{z+} \Leftrightarrow (\equiv AlOH_2)LM^{z+1-n} \qquad (E.\ 22)$$

SURFACE COMPLEXATION MODEL				
γ-Al_2O_3	2 Al[3+], 3 H_2O, -6 H[+]	logK = -16		this work
Surface sites	**BET = 136 $m^2 \cdot g^{-1}$**			
site S_w-OH	density = 1.1 $\mu eq \cdot m^{-2}$			[20]
site S_s-OH	density = 0.001 $\mu eq \cdot m^{-2}$			this work
SURFACE ACIDITY				
S_w-O[-]	1 S_w-OH, -1 H[+]	logK = -9.7		[20]
S_w -OH_2[+]	1 S_w -OH, +1 H[+]	logK = 6.9		[20]
S_s-O[-]	1 S_s-OH, -1 H[+]	logK = -8.5		this work
S_s-OH_2[+]	1 S_s -OH, +1 H[+]	logK = 6.5		this work
ANION COMPLEXES	**DEFINITION**	**logK**		
$S_{w/s}$-OH_2ClO_4	1 $S_{w/s}$-OH, +1 H[+], 1 ClO_4[-]	8,5		[20]
$S_{w/s}$-OH_2NO_3	1 $S_{w/s}$-OH, +1 H[+], 1 NO_3[-]	9,5		[20]
$S_{w/s}$-OH_2HCO_3	1 $S_{w/s}$-OH, +1 H[+], 1 HCO_3[-]	11,5		[20]
$S_{w/s}$-OH_2SO_4[-]	1 $S_{w/s}$-OH, +1 H[+], 1 SO_4[2-]	12,3		[20]
$S_{w/s}$-OH_2Cl	1 $S_{w/s}$ -OH, +1 H[+], 1 Cl[-]	9,2		[24]
MODEL 1 discarded*	**2 sites / 1sorbed species Cd^{2+}**	**1A**	**1B**	
S_s-OCd[+]	Al_s-OH, -1 H[+], 1 Cd[2+]	1,85	1,6	discarded
S_w-OCd[+]	S_w-OH, -1 H[+], 1 Cd[2+]	-1,9	-2,6	discarded
MODEL 2	**2 sites / 2 sorbed species**			
S_s-OCd[+]	S_s-OH, -1 H[+], 1 Cd[2+]	1,6		this work
S_w-OCd[+]	A_w-OH, -1 H[+], 1 Cd[2+]	-2,7		this work
S_w-OCdOH	A_w-OH, -2 H[+], 1 Cd[2+], 1 H_2O	-12,5		this work
Empirical Kd	At acidic conditions	2 $mL \cdot g^{-1}$		this work
POSSIBLE CD-ANION SPECIES	**NON ACCEPTABLE IN NON-ELECTROSTATIC MODEL**			
$S_{w/s}$-OH_2-n(ClO_4)-Cd	S_w-OH, 1 Cd[2+], 1 H[+], n ClO_4[-]	(n = 1) 12.0 (n = 3) 14.2		this work
$S_{w/s}$-OH_2-(SO_4)-Cd[+]	S_w-OH, 1 Cd[2+], 1 H[+], 2 SO_4[2-]	18,2		this work
DISCARDED COMPLEXES				
S_w-OH_2-$CdCl_3$	S_w-OH, 1 Cd[2+], 1 H[+], 3 Cl[-]	20,3		discarded
Bidentate $(S_w\text{-}O)_2$-Cd	2 S_w-OH, -2 H[+], 1 Cd[2+]	-10,5		discarded

*Table 4. Surface complexation model. *Model 1 was discarded, and **Model 2 needed to be improved with additional complexes: considered and discarded ones.*

4 EXPERIMENTAL RESULTS

4.1 ALUMINA NANOPARTICLES CHARACTERISATION

The characterization of selected γ-Al_2O_3 nanoparticles aimed to complement previous studies conducted in [20].

The oxide phase was verified by XRD analyses. Figure 2 shows the obtained XRD spectrum. Diffraction analyses confirmed that the selected aluminium oxide is gamma phase (γ-Al_2O_3) in distorted tetragonal phase, not in the usual cubic phase, what suggested that their synthesis was carried out by calcination of bohemite or gibbiste [40].

Particle size was measured by AFM. Figure 3 shows an AFM image of γ-Al_2O_3 NPs, initially suspended in $NaClO_4$, deposited and dried in a mica sheet with poly-L-lysine. It can be appreciated that single alumina particles have a mean size <50 nm, but they form aggregates with a size around 100–250 nm. The minimum hydrodynamic size measured by PCS, conditions that favour disaggregation (at the lowest ionic strength and pH far from the point of zero charge) was around 280 ± 10 nm [20] .

Zeta-potential measurements showed independence on the ionic strength, presenting the isoelectric point of the oxide (pH_{IEP}) near 8.5 [20].

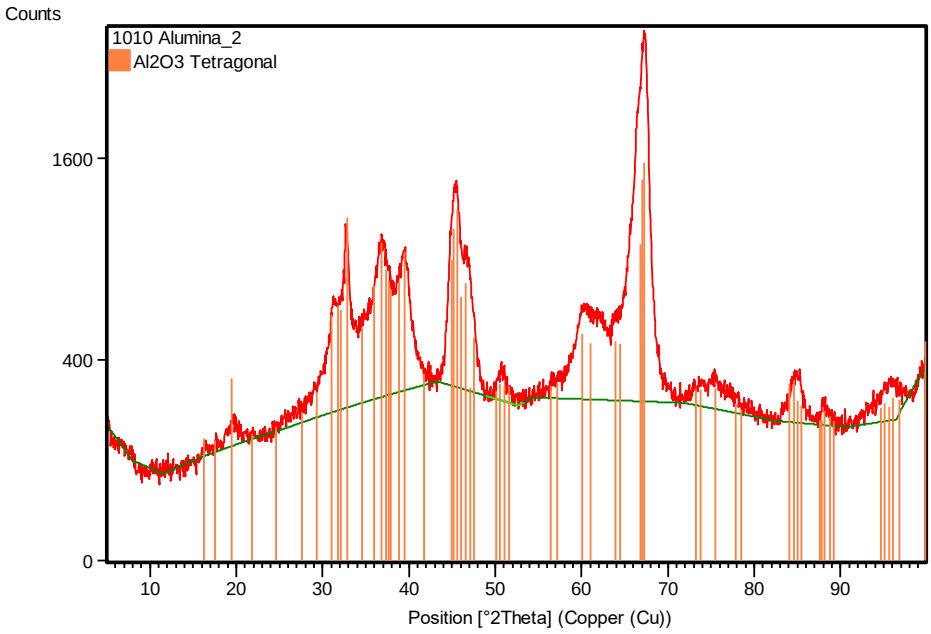

Figure 2. XRD diagram of Al_2O_3 nanopowder which confirmed the gamma oxide phase [40].

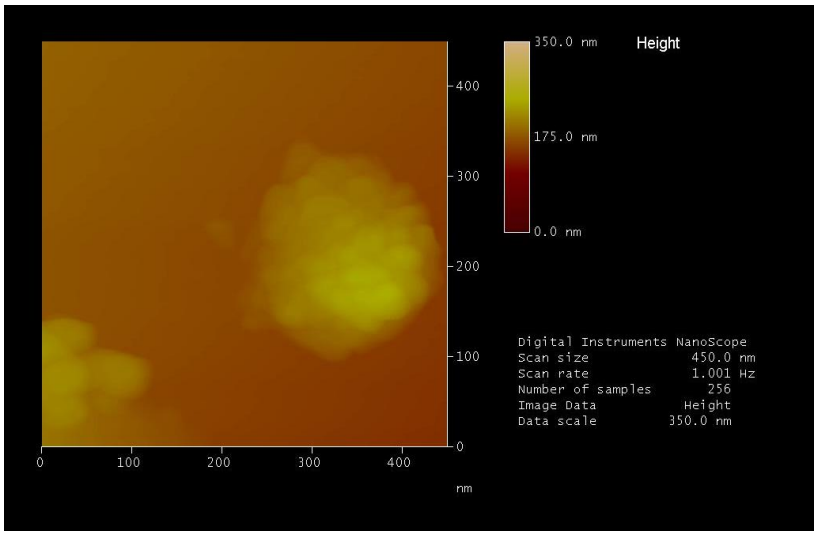

Figure 3. AFM image of γ-Al_2O_3 NPs prepared in $NaClO_4$ at pH 9, deposited and dried on a mica sheet.

4.1.1 SOLID DISSOLUTION: SOLUBILITY PRODUCT

Figure 4 shows measured Al^{3+} concentration dissolved from γ-Al_2O_3 NPs in 10^{-3} M $NaClO_4$, at different pH and contact times. At fix pH, very similar dissolved Al concentrations were measured with time and, as expected, higher dissolution is measured at acidic (pH ~ 3) or alkaline conditions (pH ~ 11).

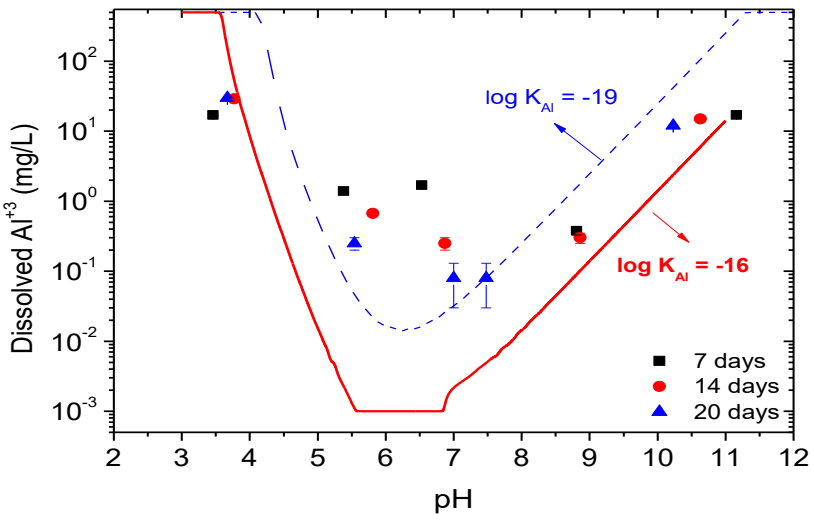

Figure 4. Dissolved Al^{3+} from γ-Al_2O_3 NPs in $NaClO_4$ 10^{-3} M, at different pH and contact time. Fit considering solubility product $logK_{Al}$ = -19 is plotted as dashed line, selected fit is plotted as continuous line ($logK_{Al}$ = -16).

Al^{3+} dissolution data was fitted as described in section 2.1.1. Different solubility products were considered. The selection of a low solubility constant ($logK_{Al}$ = -19) provided a reasonable fit within neutral pH region, but significantly overestimates the dissolution at acidic and alkaline conditions, even predicting complete dissolution. Considering that full dissolution was not observed in sorption experiments, it was decided to better adjust data at acidic and basic conditions, and the best fit was achieved with a $logK_{Al}$ = -16. Selected solubility product (log K_{Al} = -16) is within

reported values for equivalent alumina phases.: $logK_s$ = -14.37 [41], $logK_{s=}$ -14.82 [42], $logK_{s=}$ -18.89 [43]; $logK_{s=}$ -19.14. In general, higher values are reported for γ- Al_2O_3 phases obtained at higher temperatures [44], what would be in agreement to XRD analyses, that suggested synthesis by calcination (Figure 2).

4.1.2 POTENTIOMETRIC TITRATION

Figure 5 shows the titration data reported in [20] re-simulated incorporating γ-Al_2O_3 dissolution, considering the solubility constant obtained (log K_{Al} = -16) and including Al hydrolysed species whose equations and constants [29, 38] were included in Table 3.

It was observed that the revised fitting (blue line) was very similar to previous one (red line), just showing differences for pH > 10. It has to be noted that a lower solubility constant (log K_{Al} = -19) did not fit experimental titration, even modifying pKs, which again supports the solubility product selection (log K_{Al} = -16). Previously reported acidity constants (pK_{a1} = -6.9, pK_{a2}= 9.7) and density of surface sites (1.1 μeq·m^{-2}) were maintained.

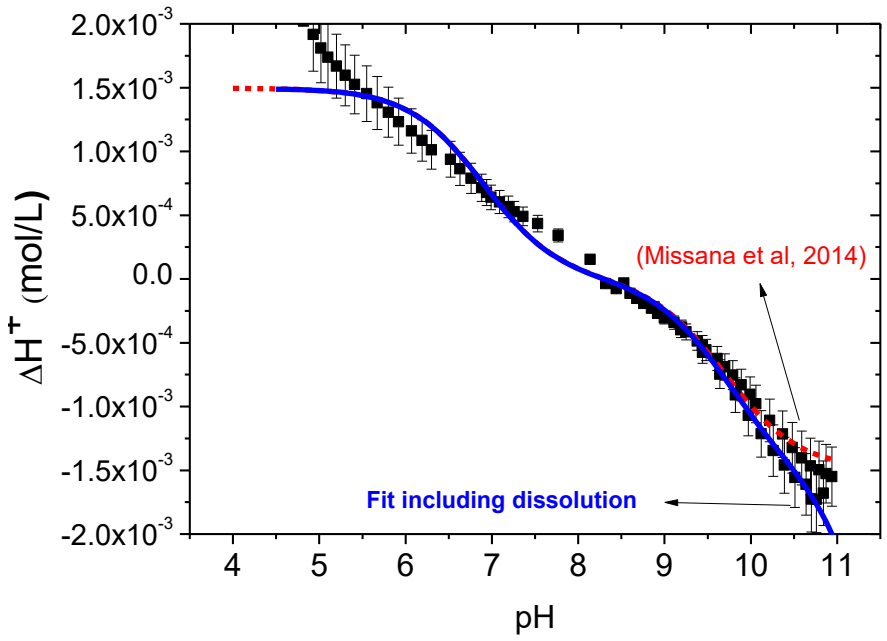

Figure 5. Potentiometric titration of γ-Al_2O_3 NPs reported in [20] with: (red line) previous fit and with (blue line) revised fir incorporating Al dissolution and hydrolysis.

4.2 CADMIUM AQUEOUS SPECIATION

Figure 6a presents, as example, a cadmium speciation diagram obtained in $NaClO_4$ 10^{-1} M, as a function of pH, considering a Cd concentration of $9.8 \cdot 10^{-6}$ M.

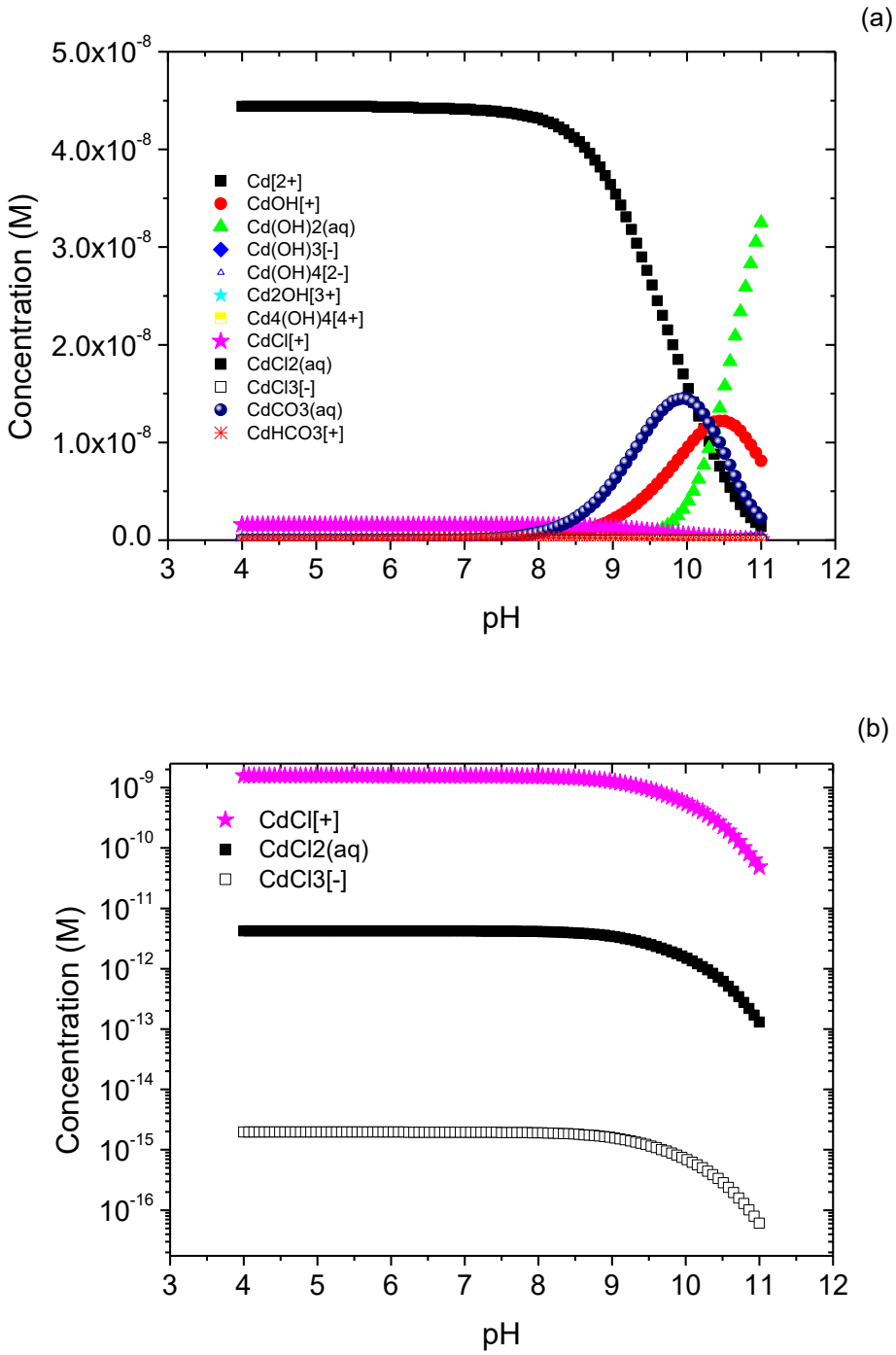

Figure 6. (a) Predicted Cd aqueous speciation in $NaClO_4$ 10^{-1} M. [Cd] = $9.8 \cdot 10^{-6}$ M, [Cl^-] = $1 \cdot 10^{-3}$ M and aqueous [HCO_3^-] = 36 mg·L^{-1}. (b) Enlargement of lower concentration region, to better appreciate predicted cadmium-chloride aqueous species.

In all model calculations, the main ions present in solution were considered. In this diagram, an average HCO_3^- concentration of 36 mg·L^{-1} and a Cl^- concentration of $1 \cdot 10^{-3}$ M were considered. The aqueous carbonate concentration is the average value measured in the suspensions, under the same conditions [24, 25]. The Cl^- concentration accounts both for the $CdCl_2$ tracer and the maximum HCl added to fix acidic conditions.

Figure 6 shows that the predominant Cd aqueous specie is Cd^{2+} up to pH 9. The predominance of Cd^{2+} species is more extended that that of other cations like for example Ni, Cu or Pb, whose carbonate- species dominate at pH around 7.5. For pH > 9, carbonate species starts playing a relevant role while for pH > 10 the first hydrolysed Cd specie ($Cd(OH)^{+}$) is dominant in solution.

In Figure 6b, the speciation diagram is limited to the lower concentration region (10^{-16} to 10^{-9} M), to better appreciate predicted cadmium-chloride aqueous: Cd-Cl aqueous complexes are at trace level.

No precipitation was detected at this Cd concentration, but at higher concentrations, under atmospheric conditions, main solids limiting Cd solubility are $CdOH_2(s)$ and otavite ($CdCO_3(s)$).

4.3 RESULTS ON CADMIUM SORPTION ONTO ALUMINA

4.3.1 CADMIUM SOPRTION KINETICS

Figure 7 presents the Cd distribution coefficient measured as a function of contact time.

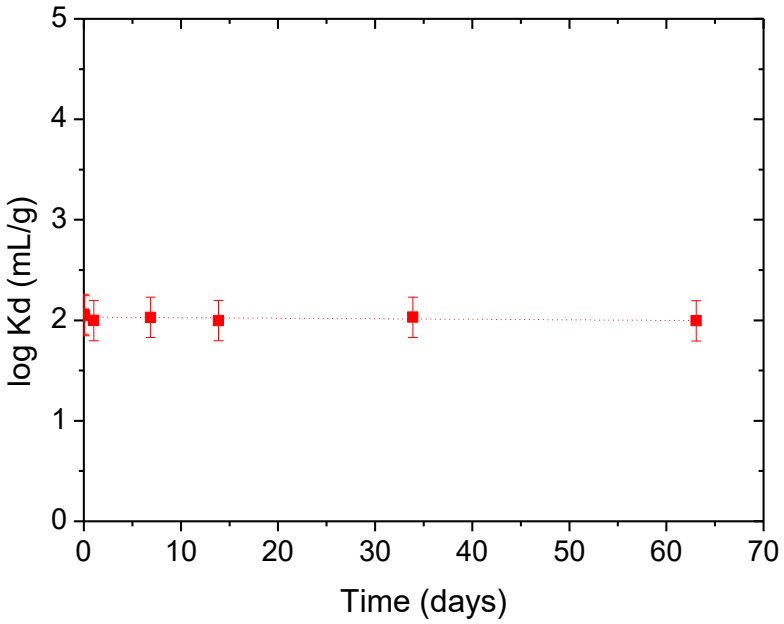

Figure 7. Distribution coefficient of Cd onto γ-Al_2O_3 measured as a function of time, in $NaClO_4$ 10^{-1} M at pH 5.5, with an initial Cd concentration of $2{\cdot}10^{-9}$ M. Solid to liquid ratio (0.5 $g{\cdot}L^{-1}$).

The kinetics of cadmium sorption onto γ-Al_2O_3 nanoparticles was checked in $NaClO_4$ 10^{-1} M at pH 5.5 with an initial Cd concentration of $2{\cdot}10^{-9}$ M. Sorption equilibrium was reached in few hours. Equilibrium time for all further sorption experiments was fixed to 1 week.

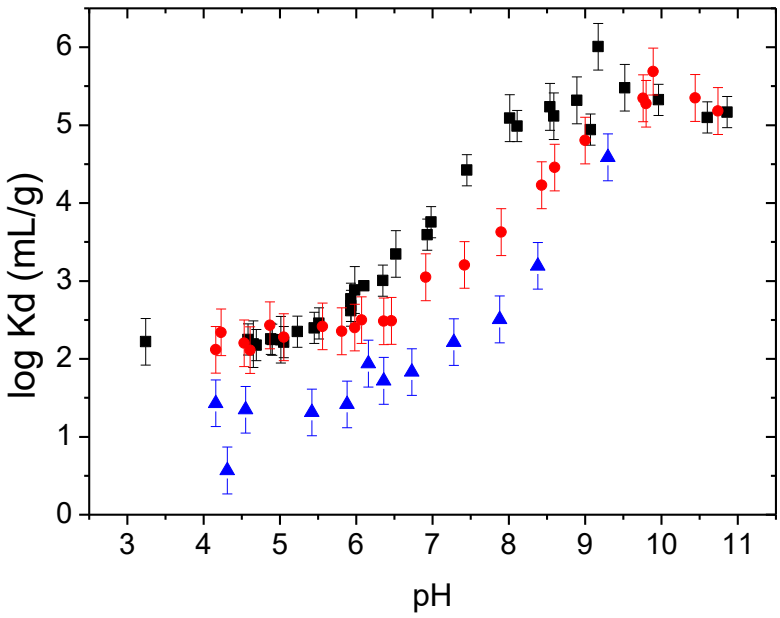

Figure 8. Cadmium sorption edges on γ-Al_2O_3 NPs in NaClO4 10-1 M, with two different Cd initial concentration (■) $4.6 \cdot 10^{-8}$ M, (●) $9.8 \cdot 10^{-6}$ M and (▲) $4.9 \cdot 10^{-4}$ M.

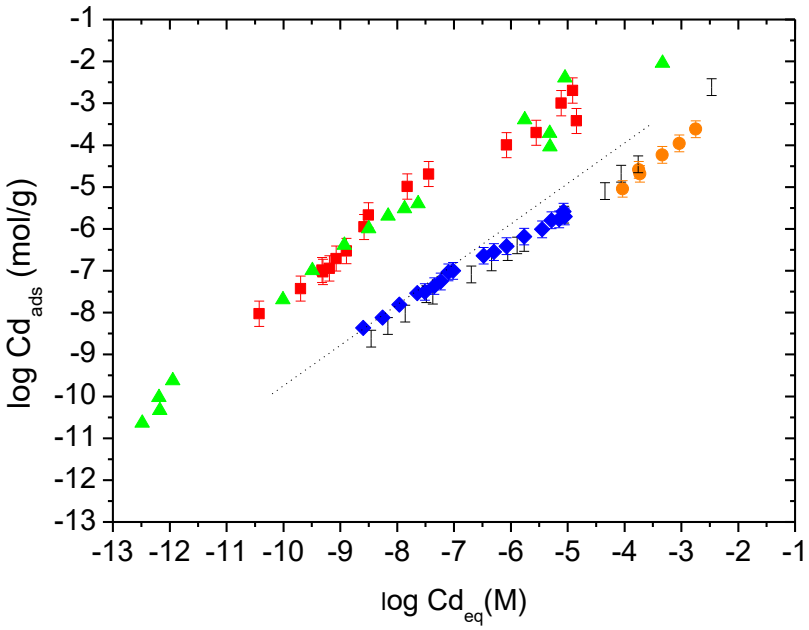

Figure 9. Cadmium sorption isotherms onto γ-Al_2O_3 NPs in $NaClO_4$ 10^{-1} M, at different pH: (◆) pH 6.1, (●) pH 6.4, (▲) pH 8.9 and (■) pH 9.8.

4.3.2 CADMIUM SORPTION EDGES AND ISOTHERMS

Figure 8 presents three Cd sorption edges obtained on γ-Al_2O_3 NPs in $NaClO_4$ 10^{-1} M, with different initial Cd concentration ($4.6 \cdot 10^{-8}$ M, $9 \cdot 10^{-6}$ M and $4.9 \cdot 10^{-4}$ M). The solid to liquid ratio was 0.5 $g \cdot L^{-1}$ and the contact time 7 days. Results are expressed as the logarithm of distribution coefficient as function of pH.

For pH higher than 5, Cd distribution coefficient showed strong pH dependence, as expected for cation sorption on an oxide surface. Higher sorption is clearly measured at lower Cd initial concentration, what suggested the existence of two sorption sites with different Cd affinity on the Al_2O_3 surface. Moreover, it was noteworthy that unexpected Cd sorption was measured for pH lower than 5, as it was observed for Sr sorption on the same alumina [25].

Figure 9 shows Cd sorption isotherms obtained on Al_2O_3 NPs in $NaClO_4$ 10^{-1} M at different pH (6.1, 6.4, 8.9 and 9.8). Results are expressed as the logarithm of the the logarithm of the Cd concentration adsorbed per gram of solid (Cd_{ads} in $mol \cdot g^{-1}$) *vs.* cadmium concentration measured in the liquid phase at equilibrium (Cd_{eq}, in mol L^{-1}). The slope of the log-log plot is lower than 1 (slope 1 is indicated as a dotted line in the figure), what suggests sorption of two Cd species or the existence of more than one sorption site is expected.

4.3.3 IONIC STRENGTH DEPENDENCE

Figure 10 shows Cd sorption edges on γ-Al_2O_3 NPs at different ionic strengths (10^{-1}, 10^{-2} and 10^{-3} M) in $NaClO_4$. The dependence of Cd sorption on ionic strength, in $NaClO_4$ is very little.

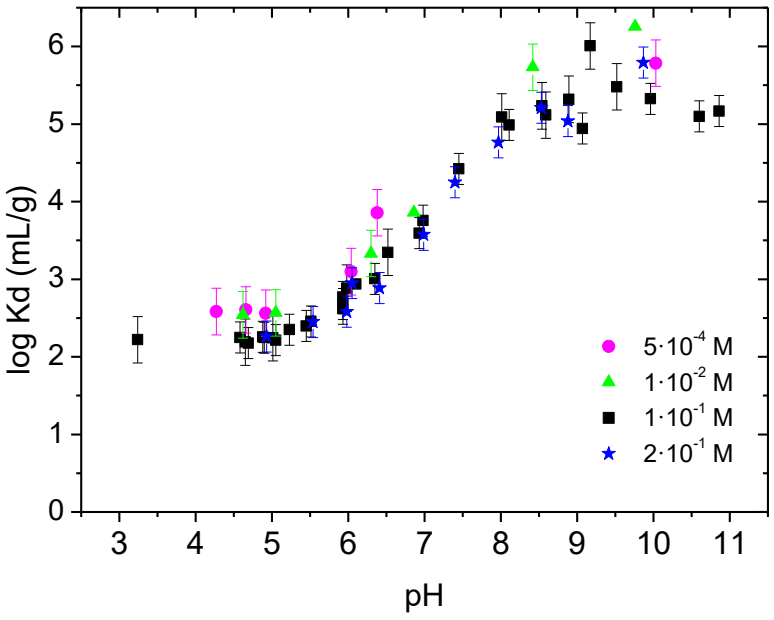

Figure 10. Cadmium sorption on γ-Al_2O_3 NPs as a function of pH in $NaClO_4$ at different ionic strength: (●) $5 \cdot 10^{-4}$ M, (▲) $1 \cdot 10^{-2}$ M, (■) $1 \cdot 10^{-1}$ M and (★) $2 \cdot 10^{-1}$ M. Cadmium initial concentration is $4.6 \cdot 10^{-8}$ M.

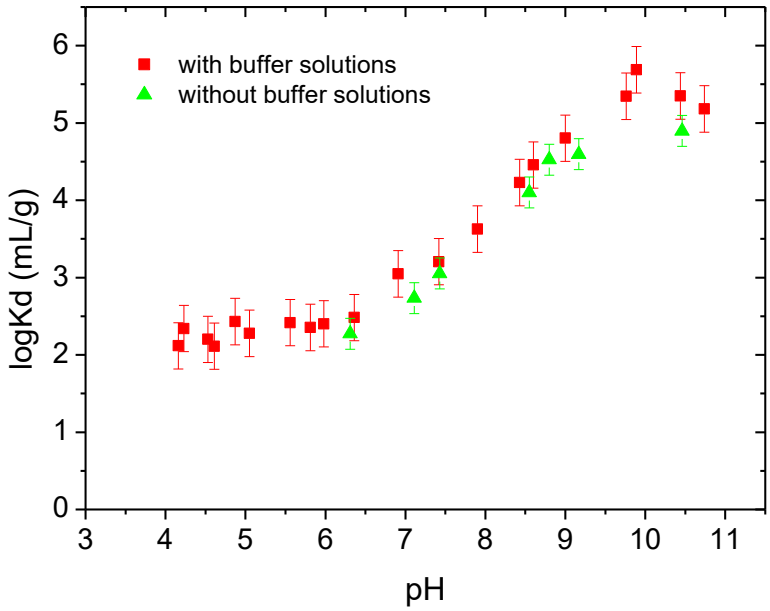

Figure 11. Cadmium sorption edges on γ-Al_2O_3 NPs in $NaClO_4$ 10^{-1}M with or without addition of buffer solutions to maintain pH. Cd initial concentration was $9.8 \cdot 10^{-6}$ M.

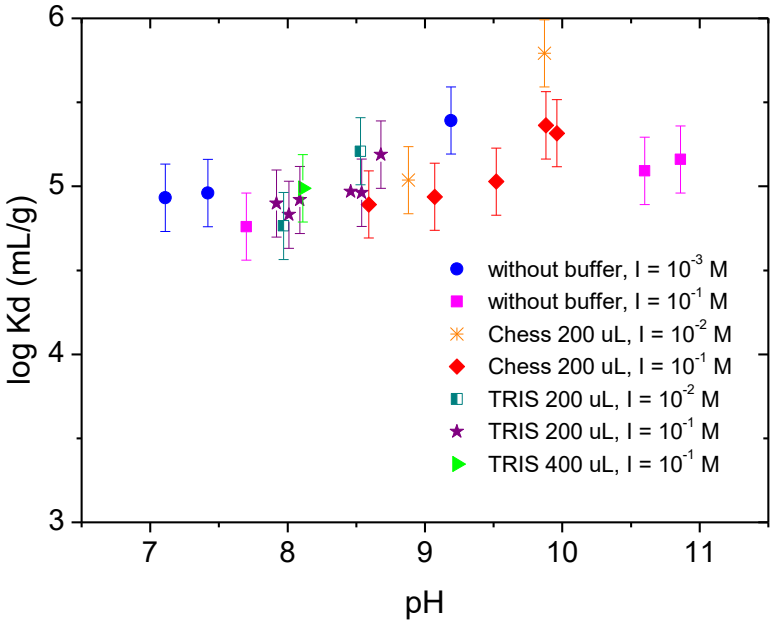

Figure 12. Cd distribution coefficients measured in γ-Al_2O_3 suspensions in $NaClO_4$ at different ionic strengths (10^{-3}, 10^{-2} and 10^{-1} M), without any buffer or with different quantities (200 or 400 μL) of TRIS or CHESS buffer solutions.

4.3.4 BUFFER EFFECTS ON CADMIUM SORPTION

As mentioned in the experimental section, different buffer solutions were used to maintain the pH, and it was verified whether they have an effect on Cd sorption.

Figure 11 shows Cadmium sorption edges on Al_2O_3 NPs in 10^{-1} M $NaClO_4$ with or without buffer solutions to adjust pH. It can be seen that sorption edges are equivalent at most pH.

A detailed analysis of buffer effects was carried out within the pH region from 7 to 11. Figure 12 shows distribution coefficients measured onto γ-Al_2O_3, prepared without any buffer or with different buffers (TRIS, CHESS) and concentrations (200 or 400 μL). It can be appreciated that measured values are very similar, within experimental errors, so that buffer effects on Cd sorption can be discarded.

4.3.5 PRE-HYDRATION EFFECTS ON CADMIUM SORPTION

One of the most noticeable results of these experiments was to find remarkable Cd sorption within acidic pH region (pH 3 to 5), which was mostly independent on pH and on ionic strength (Figure 10). Effects due to sampling or centrifugation were discarded since some samples were ultra-centrifuged (245000 g during 30 min) and results were totally equivalent. Moreover, no significant Cd sorption on centrifuge tubes was neither detected.

We wondered if these effects could be due to alumina hydration and incorporation of anions present in solution. To verify this, Cd sorption was analysed on alumina suspensions pre-hydrated in deionised water.

Figure 13 presents Cd distribution coefficients measured within pH 4 to 5 on alumina suspensions differently prepared. Two suspensions were directly prepared in $NaClO_4$ (at two different ionic strengths), other suspension was pre-hydrated in deionised water and after one day $NaClO_4$ was added, and the last one was directly suspended in deionised water. In all cases CdCl was spiked after one day of contact. It can be seen that measured Cd distribution coefficients are fully equivalent, so that the hydration procedure is not playing a relevant role.

4.3.6 ALUMINA AGGING LUMINA AGING EFFECTS ON CADMIUM SORPTION

Possible aging effects γ-Al_2O_3 nanoparticles were considered, since some authors reported that transformation to gibbsite phases may take place modifying sorption conditions [28].

Figure 14 presents the comparison of Cd distribution coefficient measured on γ-Al_2O_3 hydrated during a few hours or during 1 month. It can be seen that Cd sorption is completely equivalent, so that aging effects at the Al_2O_3 surface, within our experimental times can be discarded.

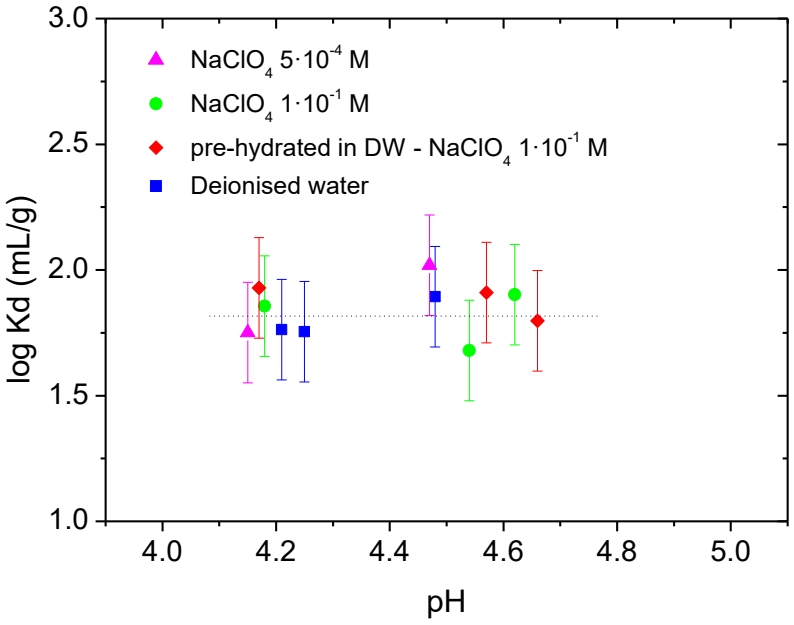

Figure 13. Comparison of Cd distribution coefficients on γ-Al_2O_3 suspensions differently prepared: (▲) suspended in $NaClO_4$ $5\cdot10^{-4}$ M, (●) suspended in $NaClO_4$ 10^{-1} M, (◆) Pre-hydrated din deionised water and after adding $NaClO_4$ 10^{-1} M and (■) prepared in deionised water. Initial Cd concentration [Cd] = $4.6\cdot10^{-8}$ M, solid to liquid ratio 0.5 $g\cdot L^{-1}$:

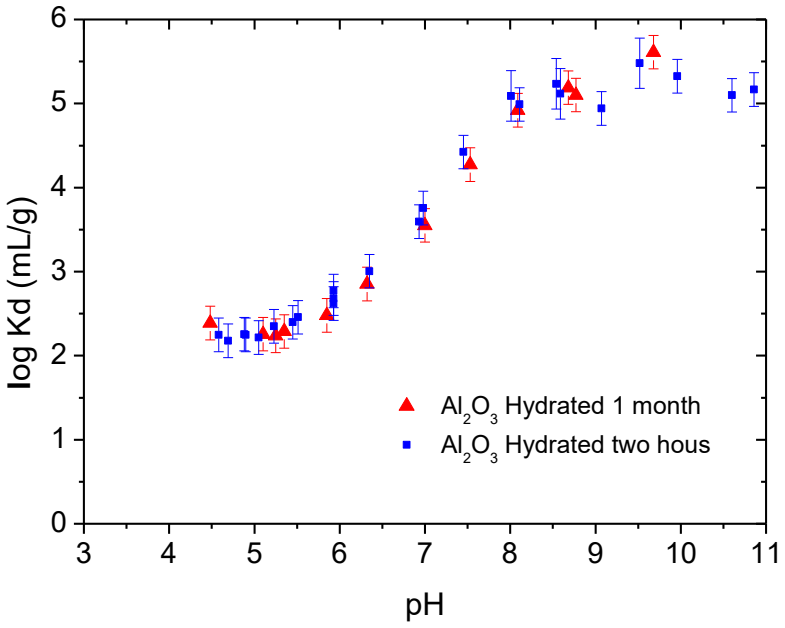

Figure 14. Cadmium sorption measured $NaClO_4$ 10^{-1} M with Cd initial concentration of $4.6\cdot10^{-8}$ M on Al_2O_3 NPs previously hydrated (■) 2 hours (▲) 1 month.

4.3.7 CHLORIDE EFFECT OF CADMIUM SORPTION

There is controversy regarding the need to account for Cd- Cl complexes to describe Cd sorption on Al_2O_3 surface. Some authors considered that cation adsorption is promoted in chloride-bearing fluids [11] and included complexation of CdCl+ on both S-OH and SO^- sites to describe Cd sorption onto alumina, pointing out that chloride non-specific adsorption lowers charge at the oxide/water interface [45].

However, Shiao et al. (1981) [8] stated that chloride complexing lowered Cd soption on Al_2O_3. Looking to sorption results obtained with other bivalent cations, or other oxides, we found that Cl independence was claimed by Weerasooriya et al (2001) [46] in Pb(II) sorption studies on gibbsite, or by Bargar et al. (1998) [47, 48] which could neither find any spectroscopic evidence for the formation of a ternary Pb–Cl^+ complex on the Al_2O_3 surface. Balistrieri and Murray (1982) [49] presented results in which the influence of Cl on Cd(II) sorption on goethite was negligible as well.

Figure 15 presents cadmium sorption edges obtained on γ-Al_2O_3 in $NaClO_4$ 10^{-1} M with different Cl concentrations: null, 10^{-8} M or 10^{-3} M, under the same experimental conditions, with Cd initial concentration of $9.8 \cdot 10^{-6}$ M. It can be appreciated that no differences on the adsorption edges can be detected even though Cl sorption in the system was very different. Thus, on the view of these results there is no need to account for Cd-chloride complexes on alumina surface to explain Cd sorption.

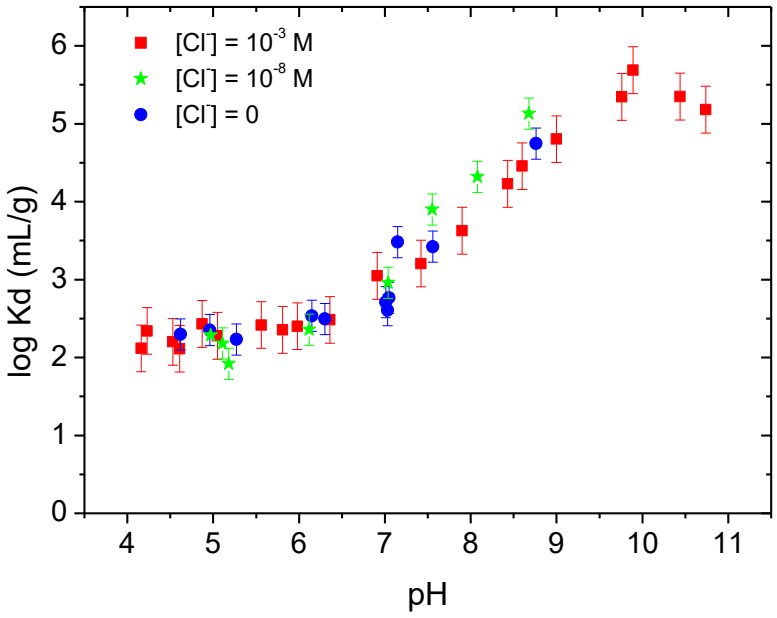

Figure 15. Cadmium sorption edges on γ-Al_2O_3 NPs in $NaClO_4$ 10^{-1}M with Cd initial concentration of $9.8 \cdot 10^{-6}$ M. Experiments were carried out with different Cl^- concentration: (■) $1 \cdot 10^{-3}$ M (★) $1 \cdot 10^{-8}$ M and (●) no Cl^-.

4.3.8 CADMIUM SORPTION ON ALUMINA IN DIFFERENT ELECTROLITES

4.3.8.1 (Hydrogen)carbonate

Figure 16 presents Cd sorption results on Al_2O_3 NPs, as a function of pH measured in $1 \cdot 10^{-1}$ M $NaClO_4$ with different concentration of bicarbonates in solution. Experiments carried out under anoxic conditions, inside a glove box, are compared to those normally carried out at atmospheric conditions or to suspensions were high bicarbonate concentrations (HCO_3 10^{-2} M or 10^{-1} M) were added, within their prevalence pH region (pH 7 to 9).

It can be appreciated that the addition of low carbonate concentration has limited effect on Cd sorption, but only at very high carbonate concentration (10^{-1} M) Cd sorption decreases. This discarded the need to include Cd-carbonate complexes in the surface complexation model. Considering that previous results confirmed that carbonate ions are absorbed on the alumina surface, the lowered Cd sorption at the highest bicarbonate concentrations occurred as it was confirmed in [20, 26] it is due to the occupation of the available surface sites. In that sense the (ir)reversibility of anion sorption may play an important role.

4.3.8.2 Nitrates

Figure 17 presents comparison of Cd sorption on Al_2O_3 NPs, as a function of pH measured in $1 \cdot 10^{-3}$ M $NaClO_4$ or $NaNO_3$. Both sorption edges are comparable, so that strong effects of NO_3^- ions on Cd sorption can be can be neglected. No Cd-NO_3 ternary complexation on Al_2O_3 surface has been also postulated by Kosma et al. (2009) [12].

4.3.8.3 Sulfates

Figure 18 shows Cd distribution coefficients measured on Al_2O_3 NPs as a function of pH in $NaClO_4$ or Na_2SO_4 at 10^{-3} M.

In principle, similar Cd sorption is measured in both electrolytes, but considering the higher affinity of $SO4^{2-}$ to alumina surface [20], in the model we will consider the inclusion of Cd-SO_4 ternary complexes, as proposed in other studies [12], that also concluded that electrolyte ions influences Cd uptake in a non-obvious way forming ternary Cd surface complexes at lower pH.

Presence of PO_4^{2-} was not considered in this work, but it has been reported that enhances Cd sorption on γ-Al_2O_3 attributed, as well, to ternary complex formation [15].

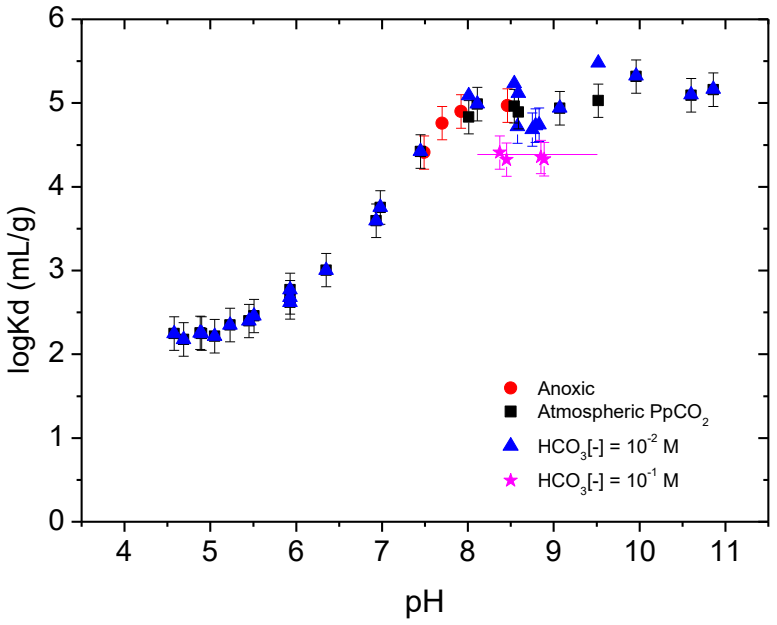

Figure 16. Cd sorption on γ-Al_2O_3 NPs in $NaClO_4$ 10^{-1} M, as a function of pH measured at: (●) anoxic conditions, (■) atmospheric conditions, (▲) HCO_3^- 10^{-2} M and (★) HCO_3^- 10^{-1} M. Cd initial concentration $4.6 \cdot 10^{-8}$ M

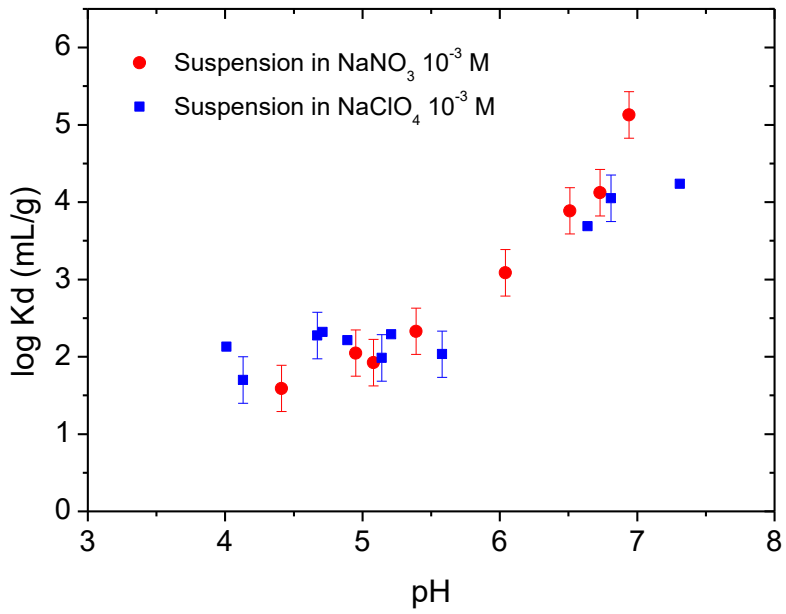

Figure 17. Cd sorption on Al_2O_3 NPs as a function of pH measured in (●) $NaNO_3$ or (■) $NaClO_4$ 10^{-3} M. Cd initial concentration $4.6 \cdot 10^{-8}$ M.

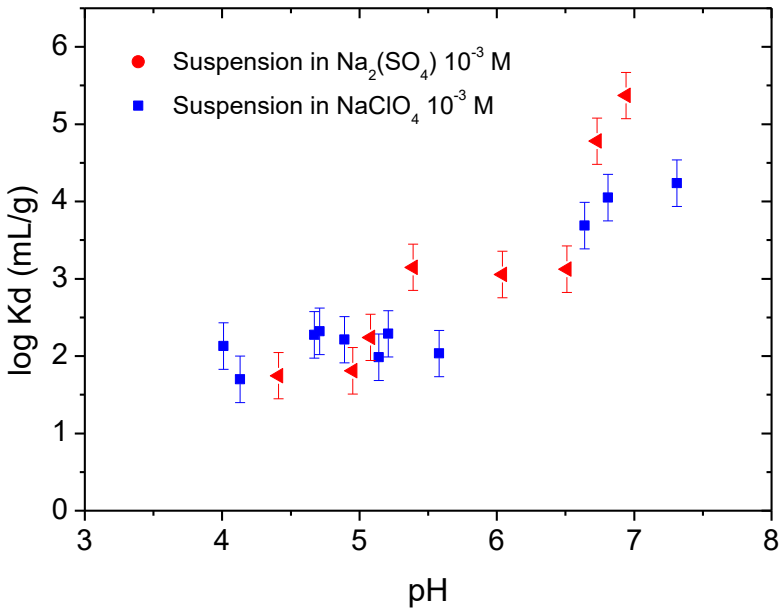

Figure 18. Cd sorption on Al_2O_3 NPs as a function of pH measured in (■) $NaClO_4$ or (◂) Na_2SO_4 at 10^{-3} M. Cd initial concentration $4.6 \cdot 10^{-8}$ M.

5 MODELLING OF CADMIUM SORPTION ON ALUMINA

Cadmium sorption was described with a non-electrostatic surface complexation model, considering two *sorption sites* on alumina surface, with different cadmium affinity, named as *strong (s) and weak (w).*

It is widely accepted that there are more than one type of aluminium surface hydroxyl group [39]. However, none of the reported Cd sorption studies onto Al_2O_3 considered a two site model, probably because none of them used low Cd concentrations ($< 10^{-6}$ M) as those used in the present work. In Floroiu et al. [16], a multisite model was neither considered, despite concentration dependence for Al-OCd complexation constant was found.

As mentioned, the site density and acidity constants of weak sites were obtained from the potentiometric titration (Figure 5) while the site density of strong sites need to be estimated form the isotherms (Figure 9), in a step-wise trial an error procedure to achieve the best fit for the experimental data.

Simplest simulation, referred as *Model 1* in Table 4 was carried out only considering complexation of Cd^{2+} on deprotonated sites, as reported by [12]. The outcome of this simplest model is presented in Figure 19 and Figure 20 which respectively show two sorption edges measured at different Cd concentration and two isotherms at two different pH (6.1 and 9.8).

Model 1A, was developed considering high Cd^{2+} complexation constants for strong and weak sites: $LogK_{Ss\text{-}OCd}$ = 1.85, $LogK_{Sw\text{-}OCd}$ = -1.9 and it is plotted as dashed line in Figure 19 and Figure 20. *Model 1A* provided a reasonable fit of Cd isotherm at pH 6, at higher Cd concentration, retention at basic conditions was clearly overestimated.

Model 1B considered lower complexation constants (*Model 1B* with $LogK_{Ss\text{-}OCd}$ = 1.6, $LogK_{Sw\text{-}OCd}$ = -2.6), and is plotted as continuous lines in Figure 19 and Figure 20. With *Model 1B* sorption edges (Figure 19) were reproduced for pH > 5, but not the isotherms (Figure 20).

Finally, the constant selected for Cd^{2+} Complex on weak sites was $LogK_{Sw\text{-}OCd}$ = -2.6, a value in agreement with values reported for Cd sorption on Al_2O_3, when single site is considered [12].

An improved model was proposed (referred as *Model 2* in Table 4) incorporation two additional surface complexes: Cd complexation on neutral >SOH sites and complexation of the first hydrolysed Cd species, $CdOH^+$ on negatively charged sites, to improve fit within the alkaline region. It is well accepted that both Cd^{2+} and $CdOH^+$ may adsorb to aluminum- and iron-oxide minerals [17].

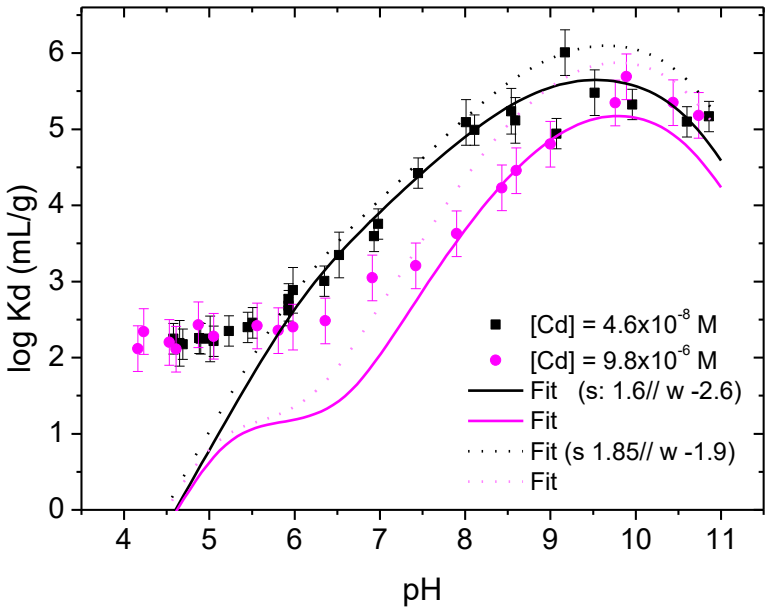

Figure 19. Cadmium sorption edges on γ-Al_2O_3 NPs in $NaClO_4$ 10^{-1} M, with two different Cd initial concentration (■) $4.6 \cdot 10^{-8}$ M and (●) $9.8 \cdot 10^{-6}$ M. Lines are fit of data with simplest model only considering Cd^{2+} complexation, accounting for different constants on strong (s) and weak(w) surface sites: Model 1A discontinuous lines, Model 1B continuous line.

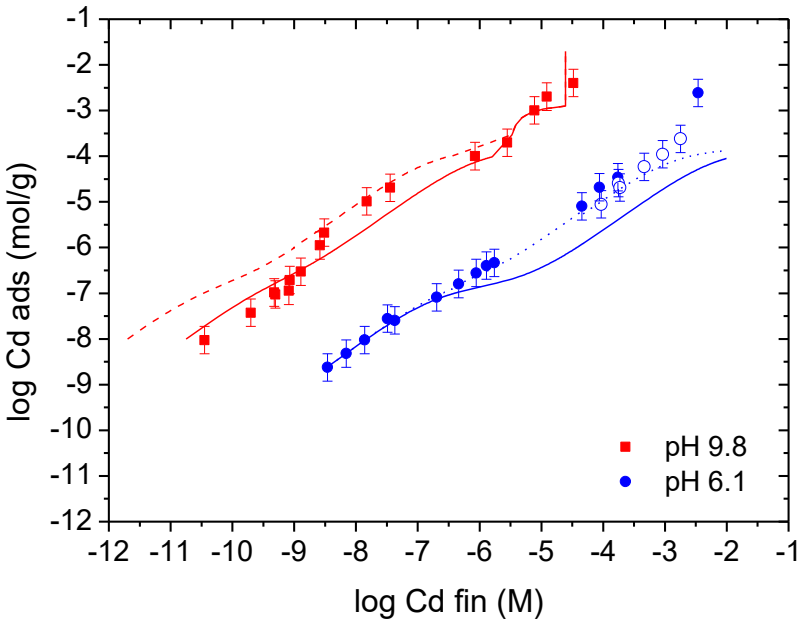

Figure 20. Cadmium sorption isotherms onto γ-Al_2O_3 NPs in $NaClO_4$ 10^{-1} M, at different pH (■) 9.8 and (●) 6.1. Dashed lines are fit of data with Model 1A and solid lines correspond to fit of data with Model 1B.

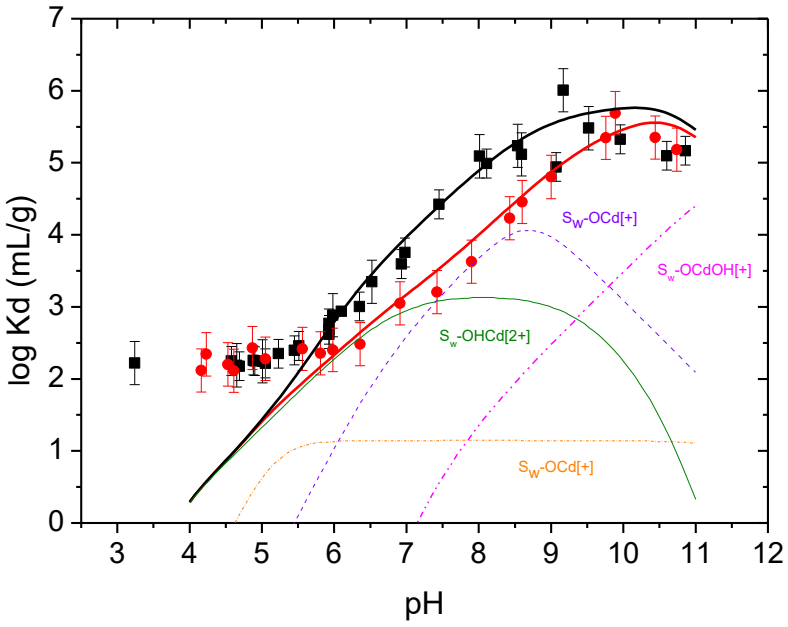

Figure 21. Simulations of two Cd sorption edges on γ-Al_2O_3 NPs in $NaClO_4$ 10^{-1} M, with two different Cd initial concentration (■) $4.6 \cdot 10^{-8}$ M and (●) $9.8 \cdot 10^{-6}$ M. Solid lines are fit of data with Model 2 (Table 4) Dashed lines correspond to the individual contribution of selected Cd complexes, determined at higher Cd concentration

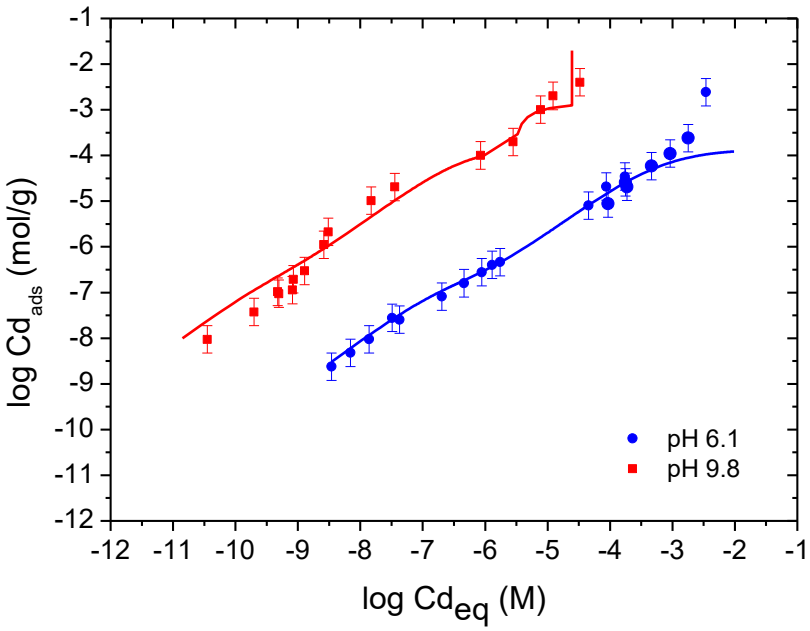

Figure 22. Simulations of Cd sorption isotherms onto γ-Al_2O_3 NPs in $1 \cdot 10^{-1}$ $NaClO_4$ M, at different pH (■) 9.8 and (●) 6.1 considering Model 2 (Table 4)

The outcome of Model 2 is shown in Figure 21 and Figure 22. *Model 2* reproduced Cd sorption edges, but only for pH higher than 5. The individual contributions of each Cd surface complex, for

the edge obtained at higher Cd concentration, are also included in the figure. In Figure 22 it is shown how *Model 2* adequately reproduced sorption isotherms.

Thus, *Model 2* did not describe, in any case, the Cd sorption systematically observed for pH values lower than 5. Cd sorption, in this acidic pH region, exhibited an average logKd of 2 ± 0.2 $mL \cdot g^{-1}$, correspondent to a 5 to 8 % Cd sorption, which is in agreement to Sr retention values measured under the same conditions on on the same alumina. In that case, modelling was carried out including an empirical logKd in the model [25].

At acidic conditions, cation sorption on Al_2O_3 surface is unexpected, since strong electrostatic repulsion with the dominant protonated surface sites would occur. Reviewing reported studies, we found that Cd sorption on γ-Al_2O_3 at acidic conditions was also observed in [9], with a Cd uptake around a 30% at pH 2.7, by [13] on activated alumina and by [50]. In contrast, other authors [16] appreciated no Cd sorption for pH < 5, in absence of Cl in solution. The US Environmental Protection Agency reported distribution coefficient for Cd sorption on soils, at acidic conditions (pH region 3-5) with an average of Kd 130 $mL \cdot g^{-1}$ [17], a value fully equivalent to our results, but giving no clue on its origin.

Many experiments were then planned to elucidate the measured Cd sorption at acidic conditions. Possible sorption onto the centrifuge tubes was verified and discarded. Experimental artefacts, due to insufficient centrifugation or to pipette sampling were discarded because they would promote particle re-suspension, increasing tracer concentration in solution and therefore diminishing the calculated sorption.

Bidentate or binary Cd complexes on Al_2O_3 surface, which were proposed by other authors on Al octahedral phases [47, 48] were considered. For example, in [11] authors included complexation of $CdCl^+$ on both S-OH and SO- sites to describe Cd sorption onto alumina, indicating that $\equiv SOCd^+$, $\equiv SOHCd2^+$ and $\equiv SOCdOH^+$, either taken alone or in combination, provide large misfits to their experimental data. However, these Cd complexes were discarded in this study. For the reader information, their definition and complexation constants are included in Table 4.

The pH-independence of Cd sorption at acid conditions, suggested the sorption of anionic species. Cd sorption within acidic region is almost independent on pH. Generally adsorption curves with shallow slopes are attributed to surface complexation reactions that do not liberate protons. The nature of this cation sorption at acidic conditions is not so easy to define. In fact,

According to speciation calculations (Figure 6), the only possible anion specie in this acid pH region would be $CdCl^3$-. The outcome of the model, incorporating complexation of $CdCl^3$ can be seen in Figure 23a.

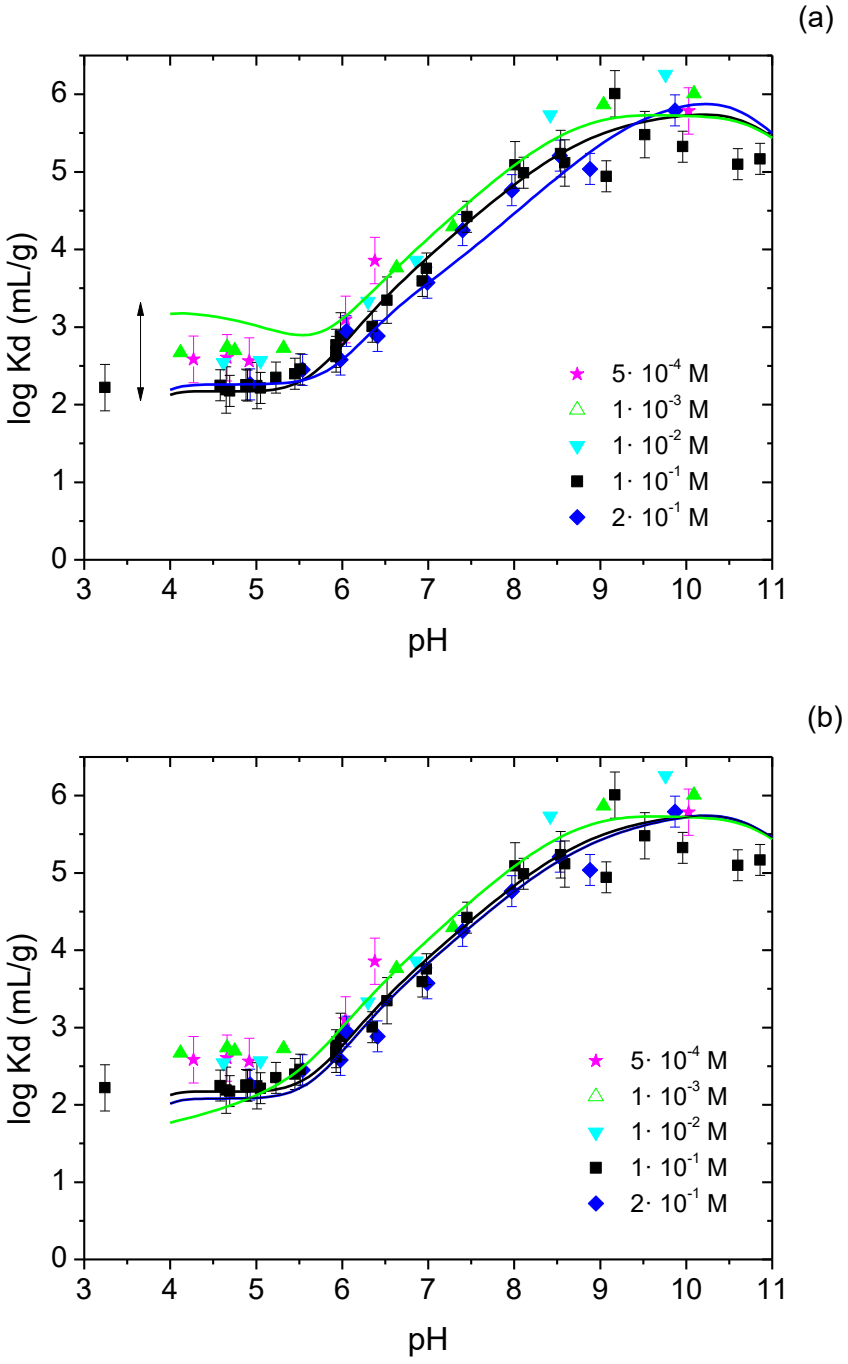

Figure 23. Ionic strength dependence of cadmium sorption on Al_2O_3 NPs in $NaClO_4$ as a function of pH. Cadmium initial concentration is $4.6 \cdot 10^{-8}$ M. Solid lines are fit considering (a) $CdCl_3$ or (b) Cd-ClO_4 complexation.

It can be seen that the edges are perfectly reproduced, considering the complexation constant for $CdCl_3$ specie included in Table 4. However, complexation of Cd-Cl was discarded because the ionic strength dependence predicted at acidic conditions is higher than measured. On top of that, the inclusion of $CdCl_3^-$ species raises the need of incorporating other Cd-chloride species.

According to speciation calculations $CdCl^+$ has exactly the same "shape" and prevalence region than Cd^{2+}, but in much lower concentration (Figure 2). However, in our case, equivalent Cd

sorption was measured in presence or in absence of Cl^- in solution, so that results did not support the inclusion of Cd-Cl complexes to describe Cd sorption onto Al_2O_3.

Thus, Cd-ClO_4 complexation was considered (Figure 23b), including the complexation constant indicated in Table 4.

It can be seen that ionic strength dependence is better reproduced. Higher electrolyte concentration results in a higher anion exchange capacity [51] and in fact, Cd-ClO_4 contribution at decreasing ionic strength can be even neglected.

Perchlorate anion is generally considered to be inert, like Na, K, Cl, or NO_3, a non-complexing ligand. In fact perchlorates are used as background electrolyte to control ionic strength [52]. Its large ionic size and low charge density reduce its affinity for metal cations and make it highly soluble and thus exceedingly mobile in natural aqueous systems. It is widely accepted that perchlorate anion is weakly adsorbed to soils, minerals, and other solid media and that, if adsorbed, it is readily and selectively displaced by a variety of Lewis bases, including phosphate, hydroxide, and silicate, among others [51].

Thus, perchlorate ions exhibited little tendency to absorb onto oxides [53]. However, perchlorate retention has been measured in variable-charge media, including studies on goethite and alumina. Sorption of perchlorate appears to occur in soils with appreciable anion-exchange capacities (AEC). A review indicates that only highly weathered soils, dominated by iron, and aluminum-oxyhydroxides and kaolinite are capable of exhibiting a significant AEC [54]. Perchlorate would be sorbed by the replacement of other anions such as chloride and sulfate [51]. Sorption of halogen ions on Al_2O_3 surface were also reported in [19]. In a previous work we provided $\equiv SOH_2$-ClO_4 complexation constant [20].

However, the inclusion of Cd-ClO_4 ternary complexes on Al_2O_3 surface brings up problems with the selection of a non-electrostatic model.

Therefore, we adopted here the same approach used to simulate Sr sorption, was to include in the model the empirical logKd measured at acidic conditions [25], and it was here adopted as well.

Figure 24 shows final simulation carried out with improved Model 2, including ternary Cd-ClO4 complexes, to Cadmium sorption edges obtained on Al_2O_3 NPs in $1 \cdot 10^{-1}$ NaClO4 M, with two different Cd initial concentration (Figure 24a) $4.6 \cdot 10^{-8}$ M and (Figure 24b) $9.8 \cdot 10^{-6}$ M. The individual contribution of selected Cd complexes is plotted as solid lines.

Figure 25 shows the simulation, carried out with the improved Model 2, to the sorption edge obtained at higher initial Cd concentration ($4.9 \cdot 10^{-4}$ M). In this case, the occupancy of alumina sites at acidic conditions, by anion ions is significate and, accordingly, Cd sorption is reduced. Moreover, under this high Cd concentration, to simulate Cd retention, otavite precipitation must be accounted for. The formation constant required to simulate this data is in agreement to values reported in [35], which are clearly different to those reported in [33]. The individual contribution of otavite precipitation is highlighted in Figure 25.

Figure 26 shows the simulations carried out with improved Model 2, to sorption isotherms carried out at four different pH. The model reproduced measured Cd retention, within the whole range of Cd concentrations analysed. The selected formation constant for otavite considered (Table 2), adequately fits measured isotherms, and Cd precipitation is detected only at high pH and high Cd concentration

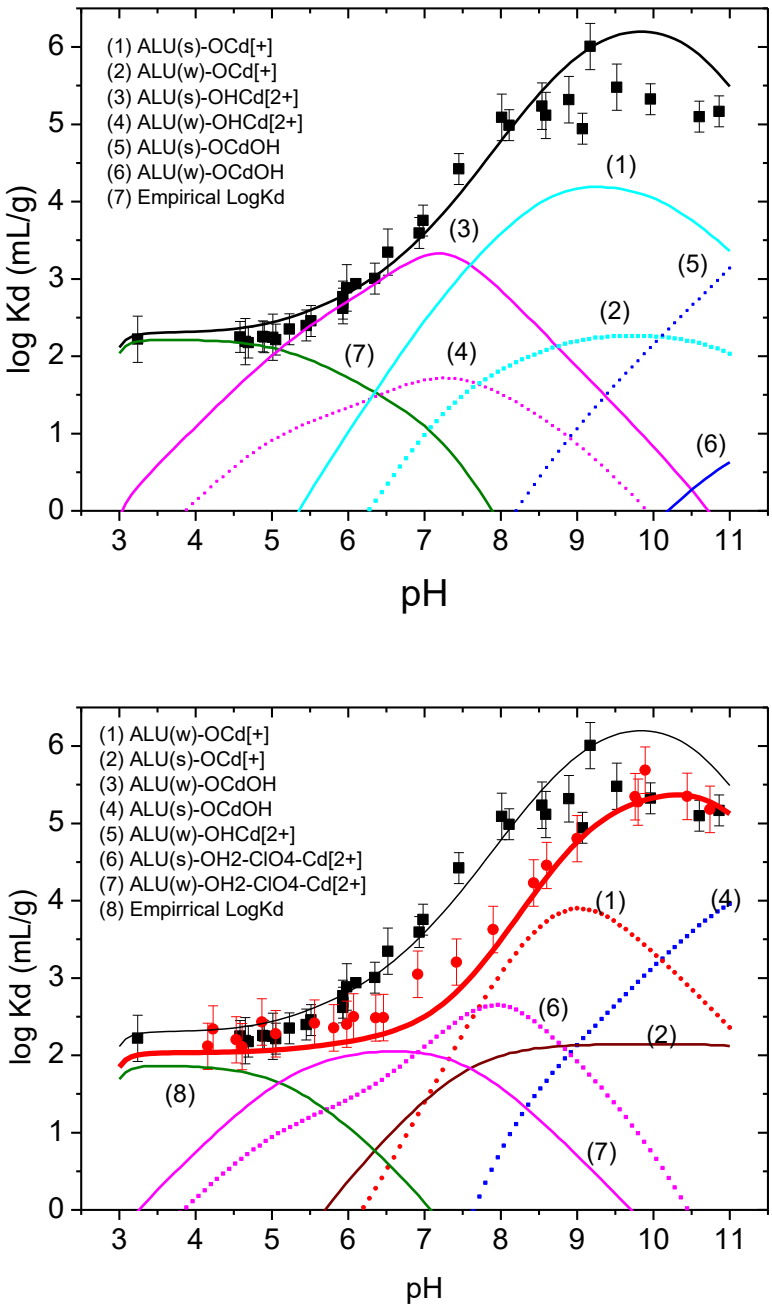

Figure 24. Simulation of Cd soprtion edges with two different Cd initial concentration (■) 4.6·10-8 M and (●) 9.8·10-6 M). Solid lines are fit of data with model 2 incorporating Cd-ClO_4 complexes.

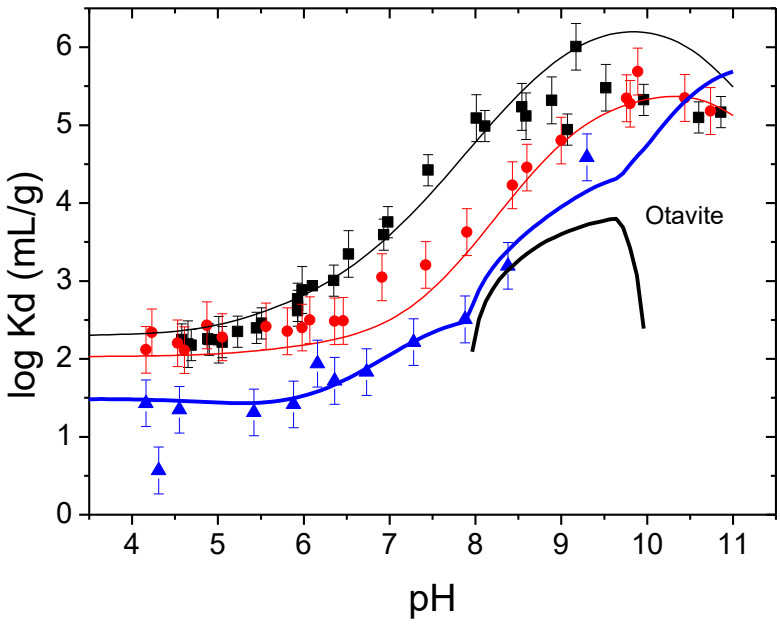

Figure 25. Simulation of Cd soprtion edges with three different Cd initial concentration (■) $4.6 \cdot 10^{-8}$ M and (●) $9.8 \cdot 10^{-6}$ M and (▲) $4.9 \cdot 10^{-4}$ M. Simulations are plotted as solid lines. The individual contribution of otavite precipitation is highlighted.

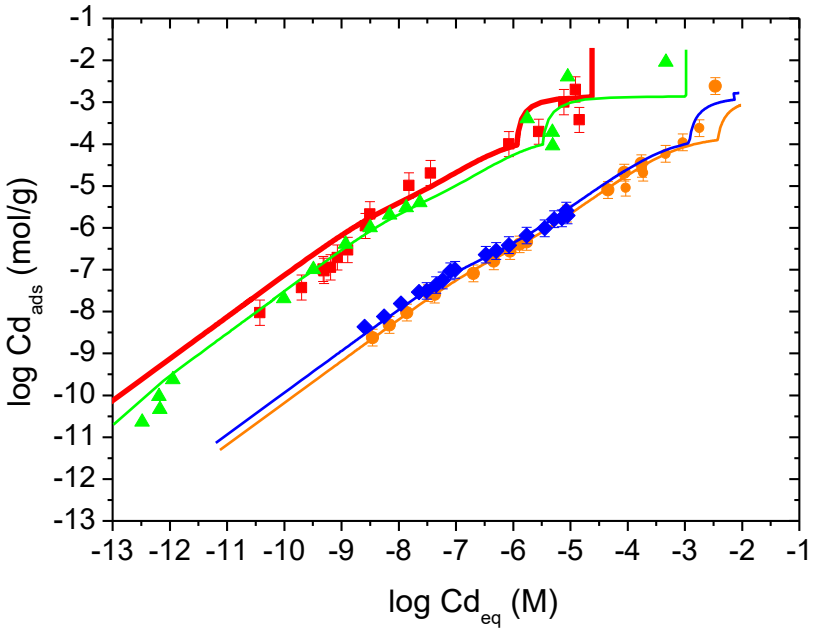

Figure 26. Cadmium sorption isotherms onto γ-Al_2O_3 NPs in $NaClO_4$ 10^{-1} M, at different pH (◆) pH 6.1, (●) pH 6.4, (▲) pH 8.9 and (■) pH 9.8. Values are expressed as logC_{ads} (mol·g^{-1}) versus logCd_{eq} (M). Lines correspond to fit of data with Model 2.

Model 2 was applied to Cd sorption data measured on alumina in other electrolytes.

Figure 27 shows the outcome of the surface complexation model for Cd experiments considering different bicarbonate concentration in solution. Fit was carried out with the Model 2, just accounting for bicarbonate competition, considering the constant reported in [20]. It can be appreciated that the observed decrease in Cd sorption is adequately predict by just incorporating bicarbonate competition.

In the same way, Figure 28 shows Cd sorption edges respectively measured in NO_3^- or ClO_4^- , which could be perfectly fitted just including competition and considering the anion constants reported in [20]. In this case, experiments were carried out at lower ionic strength ($1 \cdot 10^{-3}$ M and, as mentioned before, ternary complexation of ClO_4, and mainly NO_3, can be neglected. NO_3 ternary complexation on Al_2O_3 surface was neither claimed by other authors [12].

Figure 29 the fits carried out with Model 2 to Cd distribution coefficients measured on Al_2O_3 NPs in $NaClO_4$ or Na_2SO_4 at 10^{-3} M. Simulations just considering ClO_4^- and SO_4^{2-} competition are plotted as discontinuous lines. It can be seen that Cd sorption results measured in $NaClO_4$ are reproduced, but a lower Cd sorption is predicted at acidic conditions in Na_2SO_4. Therefore, complexation of Cd-SO_4 ternary complexes was considered (plotted as continuous line), and better fit at acidic conditions is achieved, but measured sorption was not perfectly reproduced. Selected complexation constant is slightly higher than that reported in [12], that also concluded that electrolyte ions influences Cd uptake in a non-obvious way forming ternary Cd surface complexes at lower pH. Outer-sphere complexation of SO_4 to Al_2O_3 was suggested by FTIR analyses [55].

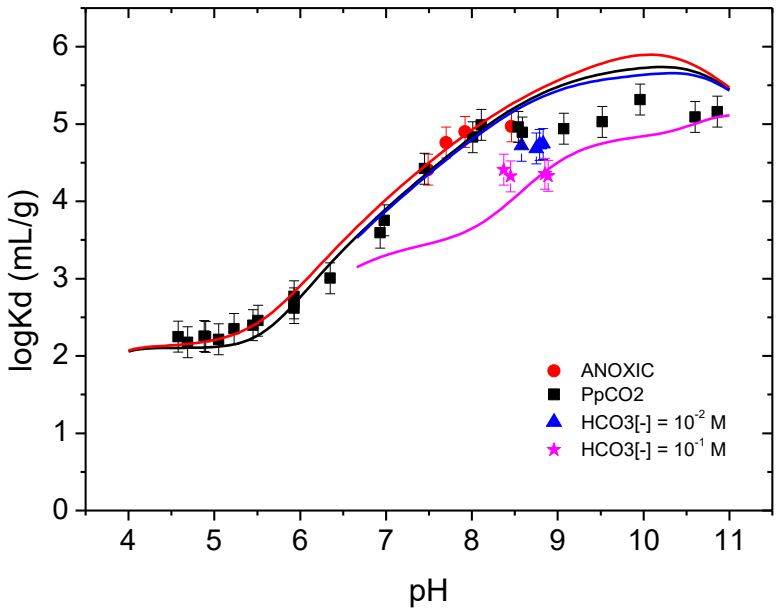

Figure 27. Simulations carried out with Model 2(Table 4) to Cd distribution coefficients measured on Al_2O_3 as a function of pH measured considering different bicarbonate concentration in solution: (■) atmospheric conditions, (▲) HCO_3^- 10^{-2} M and (★) HCO_3^- 10^{-1} M.

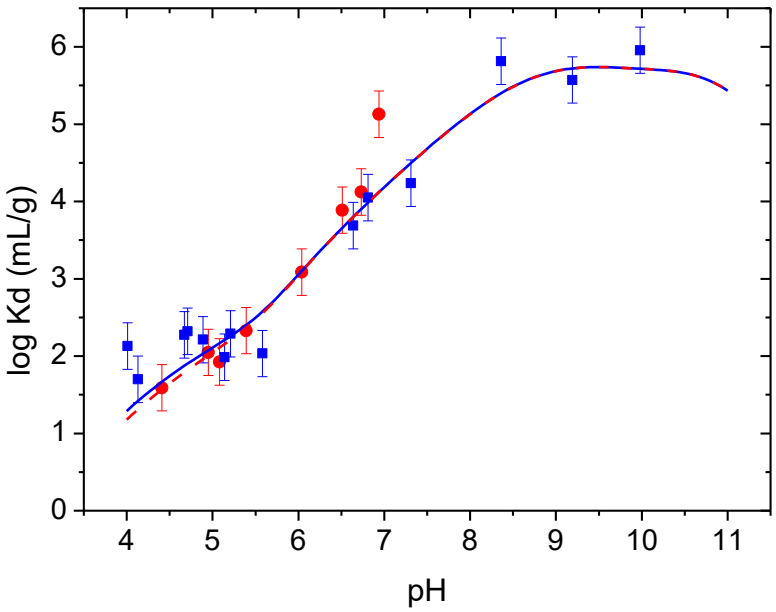

Figure 28. Simulations carried out with Model 2 (Table 4) to Cd sorption edges measured on Al_2O_3 as a function of pH measured in (●) $NaNO_3$ compared to that in (■) $NaClO_4$ 10^{-3} M.

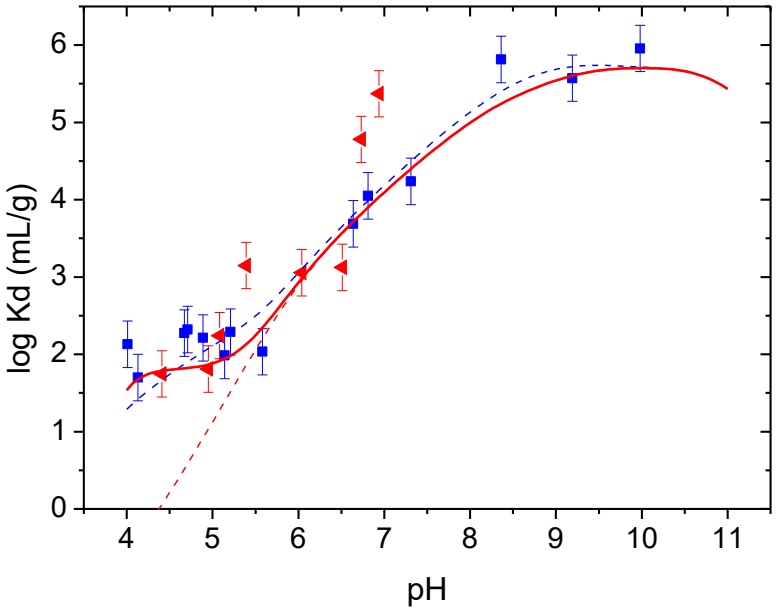

Figure 29. Simulations carried out with Model 2 (Table 4) to Cd sorption edges measured on Al2O3 in (■) NaClO4 (◀) Na2SO4 at 10-3 M. Fits considering Model 2 including ClO_4^- or SO_4^{2-} competition are plotted as discontinuous lines. Fits considering Model 2 including Cd- SO_4^{2-} complex is plotted as continuous lines.

The relevance of NO_3^-, SO_4^-, ClO_4-, Cl^- electrolyte anions on Cd uptake by γ-Al_2O_3 NPs has been probed. Presence of PO_4 was not considered in this work, but it has been reported that enhances Cd sorption on γ-Al_2O_3 attributed, as well, to ternary complex formation [15].

Overall, Cd retention on γ-Al_2O_3 surface was analysed and adequately described by a surface complexation model. Measure Cd retention capacities of this alumina, with a surface 130 $m^2 \cdot g^{-1}$, were in the range of 16 mg per gram of solid. Measured Cd capactities are within the higher values reported for equivalent oxides: 40 $mg \cdot g^{-1}$ (BET 42 $m^2 \cdot g^{-1}$) [9], 8 $mg \cdot g^{-1}$ (BET 200-300 $m^2 \cdot g^{-1}$ [10], 8.2 $mg \cdot g^{-1}$ (BET 42 $m^2 \cdot g^{-1}$) or 8.2 mg/g (BET 185 $m^2 \cdot g^{-1}$) [15]. Thus, selected γ-Al_2O_3 is a good candidate to be used in sites contaminated by Cd, to promote Cd removal.

6 CONCLUSIONS

Cadmium sorption onto gamma aluminium oxide nanoparticles was experimental and theoretically analysed by a surface complexation model (SCM).

A detailed experimental study of cadmium retention in gamma alumina has been carried out in a very wide range of experimental conditions. Experiments were mainly carried out in $NaClO_4$, and in Na_2SO_4, $NaNO_3$ and $NaHCO_3$, at different pH and ionic strengths, and in a wider range of Cd initial concentration (10^{-9} to 10^{-3} M) than previously reported. As expected, cadmium sorption was strongly pH dependent and almost independent on ionic strength.

It is worth mentioned that the comparison of Cd sorption results obtained in presence and in absence of chloride ions in solution discard the need to include complexation of Cd- chloride complexes, which was a controversial issue.

The retention capacities achieved for Cd with selected alumina, are in the range of upper values measured for equivalent oxides.

A non-electrostatic two site surface complexation model was proposed to describe Cd sorption on γ-Al_2O_3. For pH > 5, the whole set of experimental data system was well described considering complexation of Cd^{2+} on deprotonated and neutral surface sites. At basic conditions fitting had to be improved by incorporating complexation of $CdOH^+$.

Non negligible Cd sorption was systematically observed at acidic conditions in all studied electrolytes. Formation of ternary cadmium complexes with anions present in solution was hypothesized, but to maintain non-electrostatic model rigour, this contribution to Cd sorption was included in the model accounting for empirical distribution coefficient.

Proposed surface complexation model can be used to predict cadmium retention in different environments, since they are representative of aluminol sites, present in clays and in many minerals.

7 REFERENCES

[1] WHO. Exposure to cadmium: A major public health concern. WHO/CED(PHE/EPE/19.4.3. World Health Organization.; 2019.

[2] WHO. Cadmium—Environmental aspects. Geneva, World Health Organization, International Programme on Chemical Safety (Environmental Health Criteria 135) http://www.inchem.org/documents/ehc/ehc/ehc135.htm). 1992.

[3] Hutton M. Sources of cadmium in the environment. Ecotoxicology and Environmental Safety. 1983;7(1):9-24.

[4] Rao KS, Mohapatra M, Anand S, Venkateswarlu P. Review on cadmium removal from aqueous solutions. International Journal of Engineering, Science and Technology. 2010;2(7):81-103.

[5] Al-Abadleh HA, Grassian VH. Oxide surfaces as environmental interfaces. Surface Science Reports. 52(3-4) 63-161.; 2003.

[6] Strawn DG, Scheidegger A, Sparks DL. Kinetics and Mechanisms of Pb(II) Sorption and Desorption at the Aluminum Oxide-Water Interface. Environmental Science and Technology. 1998;32:2596-601.

[7] EPA. Nanotechnology for Site Remediation Fact Sheet. Environmental Protection Emergency Response. USA - EPA 542-F-08-009.; 2008.

[8] Shiao S-Y, Egozy Y, Meyer RE. Adsorption of Cs(I), Sr(II), Eu(III), Co(II) and Cd(II) by Al2O3. Journal of Inorganic Nuclear Chemistry. 1981;43(2):3309-15.

[9] Sen TK, Sarzali MV. Removal of cadmium metal ion (Cd2+) from its aqueous solution by aluminium oxide (Al2O3): A kinetic and equilibrium study. Chemical Engineering Journal. 2008;142:256–62.

[10] Asencios YJO, Sun-Kou MR. Synthesis of high-surface-area Al2O3 from aluminum scrap and its use for the adsorption of metals: Pb(II), Cd(II) and Zn(II). Applied Surface Science. 2012;258(10002-10011).

[11] Boily JF, Fein JB. Experimental study of cadmium-citrate co-adsorption onto α-AI2O3. Geochimica et Cosmochimica Acta, Vol 60, No 16, pp , 1996. 1996;60(16):2929-38.

[12] Kosma C, Balomenou G, Salahas G, Deligiannakis Y. Electrolyte ion effects on Cd2+ binding at Al2O3 surface: Specific synergism versus bulk effects. Journal of Colloid and Interface Science. 2009;331:263–74.

[13] Naiya TK, Bhattacharya AK, Das SK. Adsorption of Cd(II) and Pb(II) from aqueous solutions on activated alumina. Journal of Colloid and Interface Science. 2009;333:14-26.

[14] Plavsic M, Cosovic B. Voltammetric study of the role of organic acids on the sorption of Cd and Cu ions by alumina particles. Colloids and Surfaces A: Physicochemical and Engineering Aspects. 1999;151:189-200.

[15] Stietiya MH, Wang JJ. Zinc and Cadmium Adsorption to Aluminum Oxide Nanoparticles Affected by Naturally Occurring Ligands. Journal of Environmental Quality. 2014;43:498-506.

[16] Floroiu RM, Davis AP, Torrents A. Cadmium Adsorption on Aluminum Oxide in the Presence of Polyacrylic Acid. Environmental Science and Technology. 2001(35):348-53.

[17] EPA. Volume II - Geochemistry and Available Kd Values for Selected Inorganic Contaminants. [EPA 402-R-99-004 B]. 1999.

[18] Benjamin MM, Leckie JO. Multiple-Site Adsorption of Cd, Cu, Zn, and Pb on Amorphous Iron Oxyhydroxide. Journal of CoUoid and Interface Science. 1981;79(1):209-21.

[19] Szczepaniak W, Koscielna. H. Specific adsorption of halogen anions on hydrous Y-Al2O3. Analytica Chimica Acta. 2002;470:263–76.

[20] Missana T, Benedicto A, Mayordomo N, Alonso U. Analysis of anion adsorption effects on alumina nanoparticles stability. Applied Geochemistry. 2014;49:68-76.

[21] Missana T, Garcia-Gutierrez MJ, Rios UBAdl. Analysis and modelling of sorption processes in complex materials. Coleccion Documentos CIEMAT (Madrid, Spain). 2019.

[22] Payne TE, Brendler V, Ochs M, Baeyens B, Browne PL, Davis JA, et al. Guidelines for thermodynamic sorption modelling in the context of radioactive waste disposal. Environmental Modelling & Software. 2013;42:143-56.

[23] Mayordomo N, Foerstendorf H, Lützenkirchen J, Heim K, Weiss S, Alonso U, et al. Selenium(IV) Sorption Onto gamma-Al2O3: A Consistent Description of the Surface Speciation by Spectroscopy and Thermodynamic Modeling. Environmental Science and Technology. 2018;52(2):581-8.

[24] Mayordomo N, Alonso U, Missana T. Analysis of the improvement of selenite retention in smectite by adding alumina nanoparticles. Science of the Total Environment. 2016;572:1025-32.

[25] Mayordomo N, Alonso U, Missana T. Effects of gamma-alumina nanoparticles on strontium sorption in smectite: Additive model approach. Applied Geochemistry. 2019;100:121-30.

[26] Mayordomo N. Experimental and Theoretical Studies of Mixed Smectite and Al2O3 Nanoparticles to Improve Pollutant Retention in Geochemical Barriers. Doctoral Dissertation. Universidad de Alcalá de Henares, UAH, Madrid, Spain.; 2017.

[27] Mayordomo N, Alonso U, Missana T, Benedicto A, García-Gutiérrez M. Addition of Al2O3 nanoparticles to bentonite: effects on surface charge and Cd sorption properties. Scientific Basis For Nuclear Waste Management XXXVII Mat Res Symp Proc; 2014; 2014. p. 131-8.

[28] Karamalidis AK, Dzombak DA. Surface Complexation Modeling. Gibbsite. John Wiley & Sons, Inc.: John Wiley & Sons, Inc. 2010.

[29] Hummel W, Berner U, Curti E, Pearson FJ, Thoenen T. Nagra /PSI Chemical Thermodynamic Data Base 01/01. Parkland, Florida 2002.

[30] Baes CF, Mesmer RE. The hydrolisis of cations. Wiley Ed. 1976.

[31] van der Lee J, De Windt L. CHESS tutorial and cookbook. Technical report LHM/RD/99/05.; 1999.

[32] Zirino A, Yamamoto S. A pH-dependent model for teh chemical speciation of copper, zinc, cadmium, and lead in seawater. Limnology and Oceanography. 1972;17(5):661-71.

[33] Powell KJ, Brown PL, Byrne RH, Gajda T, Hefter G, Leuz A-K, et al. Chemical speciation of environmentally significant metals with inorganic ligands. Part 4: The Cd2+ + OH–, Cl–, CO32–, SO42–, and PO43– systems (IUPAC Technical Report). Pure and Applied Chemistry. 2011;83(5):1163–214.

[34] Gamsjäger H, Magalhães MCF, Königsberger E, Sawada K, Churagulov BR, Schmidt P, et al. IUPAC-NIST Solubility Data Series. 92. Metal Carbonates. Part 1. Solubility and Related Thermodynamic Quantities of Cadmium(II) Carbonate in Aqueous Systems. Journal of Physical and Chemical Reference. 2011;40:043104.

[35] Stipp SL, Parks GA, Nordstrom DK, Leckie JO. Solubility-product constant and thermodynamic properties for synthetic otavite, CdCO[sub 3(s)], and aqueous association constants for the Cd(II)CO[sub2]-H[sub 2]O system. Geochimica et Cosmochimica Acta. 1993;57(2699-2113).

[36] Temminghoff EJM, Zee SEATMVd, Haan FAMD. Speciation and calcium competition effects on cadmium sorption by sandy soil at various pHs. European Journal of Soil Science. 1995;46:649-55.

[37] Schulthess CP, Sparks DL. Backtitration Technique for Proton Isotherm Modeling of Oxide Surfaces. Soil Science Society American Journal. 1986;50:1406-11.

[38] van der Lee J, De Windt L. CHESS tutorial and cookbook, Technical Report LHM/RD/99/05.; 1999.

[39] Hiemstra T, Riemsdijk WHV, Bolt GH. Multisite Proton Adsorption Modeling at the Solid/Solution Interface of (Hydr)oxides: A New Approach. I. Model Description and Evaluation of Intrinsic Reaction Constants. Journal of Colloid and Interface Science. 1989;133(1):91-104.

[40] Gutierrez-Nebot L. Informe de caracterización de fases sólidas mediante XRD. Report Ref.1009 13-10-2014. Unidad Residuos Radiactivos CIEMAT, Madrid (Spain). 2014.

[41] Chen CC. Phase Equilibria at Ti–Al Interface Under Low Oxygen Pressure. Atlas Journal of Materials Science 1 (1): , 2014. 2014;1(1):1–11.

[42] Peryea FJ, Kittrick JA. Relative solubility of corundum, gibbsite, boehmite and diaspore at standard state conditions. Clays and Clay Minerals. 1988;36(5):391-6.

[43] Qiyuan C, Wenming Z, Xinmin C, Songqing G, Guanqun Y, Huifang Z, et al. Investigation of the thermodynamic properties of γ-Al2O3. Thermochimica Acta. 1995;253:33-9.

[44] Chase MW, Curnutt JL, Hu AT, Prophet H, Syverud AN, Walker LC. JANAF Thermochemical Tables. Journal of Physical and Chemical Reference Data. 1974;3(2):311-481.

[45] Gunnerisusson L. Composition and stabilityof Cd(II)-Chloro and Hydroxo Complexes at the goethite (α–FeOOH)/water interface. Journal of Colloid and Interface Science. 1994;163:484-92.

[46] Weerasooriya R, Aluthpatabendi D, Tobschall HJ. Charge distribution multi-site complexation (CD-MUSIC) modeling of Pb(II) adsorption on gibbsite. Colloids and Surfaces: A: Physicochemical and Engineering Aspects. 2001;189:131-44.

[47] Bargar JR, Jr GEB, Parks GA. Surface complexation of Pb (II) at oxide-water interfaces: I. XAFS and bond-valence determination of mononuclear and polynuclear Pb (II) sorption products on aluminum oxides. Geochimica et Cosmochimica Acta. 1997;61(3):2617-37.

[48] Bargar JR, Jr GEB, Parks GA. Surface complexation of Pb(II) at oxide-water interfaces: III. XAFS determination of Pb(II) and Pb(II)-chloro adsorption complexes on goethite and alumina. Geochimica et Cosmochimica Acta. 1998;62:193-207.

[49] Balistrieri L, Murray J. The adsorption of Cu, Pb, Zn, and Cd on geothite from major ion seawater. Geochimica et Cosmochimica Acta. 1982;46(7):1253-65.

[50] Dong Y, Liu Z, Li Y, Chen L, Zhang Z. Effect of pH, ionic strength, foreign ions, fulvic acid and temperature on 109Cd(II) sorption to γ-Al2O3. Journal of Radioanalytical and Nuclear Chemistry. 2012;292:619–27.

[51] Urbansky ET, Brown SK. Perchlorate retention and mobility in soils. Journal of Environmental Monitoring. 2003;5:455-62.

[52] Dzombak DA, Morel FMM. Surface Complexation Modeling: Hydrous Ferric Oxide.Wiley, New York. 1990.

[53] Brown GM, Gu B. Perchlorate Environmental Occurrence, Interactions and Treatment: Chapter 2. Eds Baohua Gu, &John Coates. Springer. 2006.

[54] Gu B, Schulz RK. Anion retention in soil: possible application to reduce migration of buried technetium and iodine. NUREG/CR-5464. US. Nuclear Regulatory Commission, 1991 :Washington, DC 20555. 1991.

[55] Müller K, Lefevre G. Vibrational Characteristics of Outer-Sphere Surface Complexes: Example of Sulfate Ions Adsorbed onto Metal (Hydr)oxides. Langmuir. 2011;27(6830–6835).

1135-9420